Geochemistry and Depositional Environments of the Tertiary Clays in Makkah and Rabigh Quadrangles, West Central Arabian Shield, Saudi Arabia

R.J. Taj*, N.A. Saad**, M.A. El Askary** and M.H. Basyoni*

Faculty of Earth Sciences, King Abdulaziz University
***Geology Department, Faculty of Science, Alexandria University*

ABSTRACT. The present work deals with a detailed chemical study on the clay mineral assemblages characterizing some clay deposits, shales and mudstones, which differ in their texture, colour, lithology, and depositional environments. Samples selected from seven Tertiary formations located in Makkah and Rabigh quadrangles are chemically analyzed; some are used as environmental discriminators.

The distribution of major and some trace elements in 77 samples has been investigated and the results obtained were tabulated and graphically illustrated. A wide range of variation is shown in the results of both major and trace constituents. This is due to their variable content of clay mineral constituents and the abundance or paucity of other admixtures, *e.g.* quartz, feldspar and minor heavy mineral grains. The local occurrence of minor gypsum and carbonate veinlets in some formations and ferrugination in others are also effective.

A positive correlation exists in some formations between Fe_2O_3 and each of MnO, Cr, Ni, Cu & Zn; between each of Sr & Cu versus CaO; and in most cases between Ga and Al_2O_3. Whereas SiO_2 shows a negative correlation with each of Al_2O_3 and L.O.I .

Most of trace elements entered the depositional basin in close association with clay minerals and Ca-Fe-bearing detritus.

The examined clay minerals and their trace elements are mainly source controlled (*e.g.* granitic and some pelitic rocks) and, an environmental illustration using Ga, B & Rb in a ternary diagram would

indicate transitional to marine depositional environments for the studied clay deposits.

Introduction

In the last three decades, the study of clay deposits received a great interest of some mineralogists to cope up with the expanding need of clay products. The different modes of formation and environments of clay deposition yield various clay deposits differing in their mineralogical and chemical composition, thus sharing in the diversification of clay uses (Taj *et al.,* 2001b).

The present work deals with a detailed chemical study of clays, shales and mudstones at fifty stations which represent seven Tertiary formations and four boreholes, aiming to conclude their depositional environments. They are distributed in Makkah and Rabigh quadrangles in the west central part of the Arabian Shield bordering the Red Sea between lat. 21º00' & 23º00'N and long. 38º50' & 40º30'E (Fig. 1). The selected analyzed bulk samples are seventy three from Haddat Ash Sham (HS), Usfan (US), Shumaysi (SH), Khulays (KH), Buraykah (BR), Ubhur (UB) and Dafin (DF) formations (Fig. 2). Four samples were also subjected to chemical analysis from three boreholes, located between Usfan and Haddat Ash Sham in Makkah quadrangle (Fig. 1). The distribution of the major oxides and some environmental discriminator trace elements from the clay deposits and associated mudrocks of diverse formations, has been tabulated and graphically investigated.

The used apparatuses for analyses are: computerized Perkin Elmer Mass-ICP-MS (model PQ/2) at the labs of the Geological Survey of Saudi Arabia, Jeddah; and X-ray fluorescence spectrometer (XRF) at the central laboratories sector of the Egyptian Geological Survey and Mining Authority, Giza, Egypt .

General Geology

The two quadrangles comprise Precambrian basement rocks unconformably overlain by Tertiary sedimentary rocks in the west, and by Miocene to Pliocene lavas in the north (Moore and Al- Rehaili, 1989).

Extensive areas of Quaternary surficial deposits (sand and gravel) are extended on the coastal plain and in the major wadies (Fig. 1). The stratigraphic succession of Tertiary formations, as well as, the paleogeography and structures of these sediments are studied by Spencer and Vincent (1984).

The studied formations are chronologically arranged, starting from the oldest Haddat Ash-Sham (HS), Usfan (US), Shumaysi (SH), Khulays (KH), Buraykah
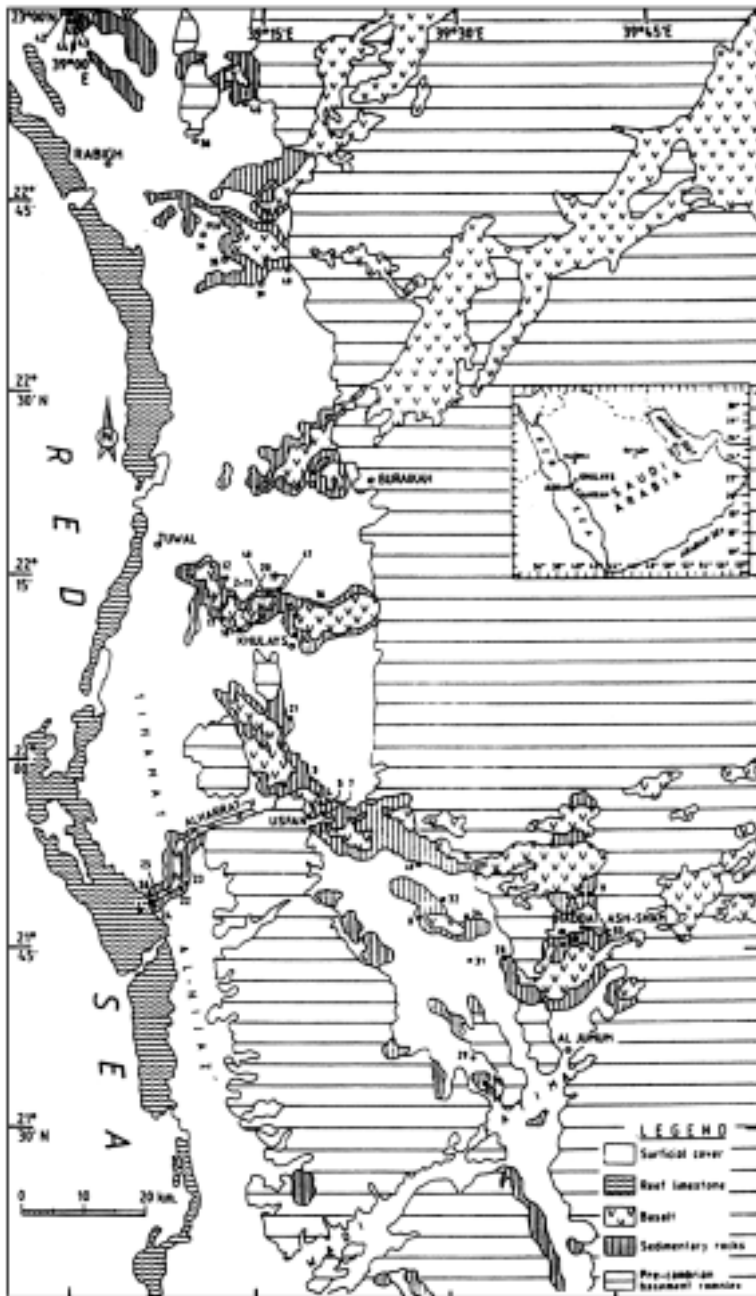
FIG. 1. Simplified geological and location map of the fifty studied stations in the Makkah and Rabigh quadrangles.
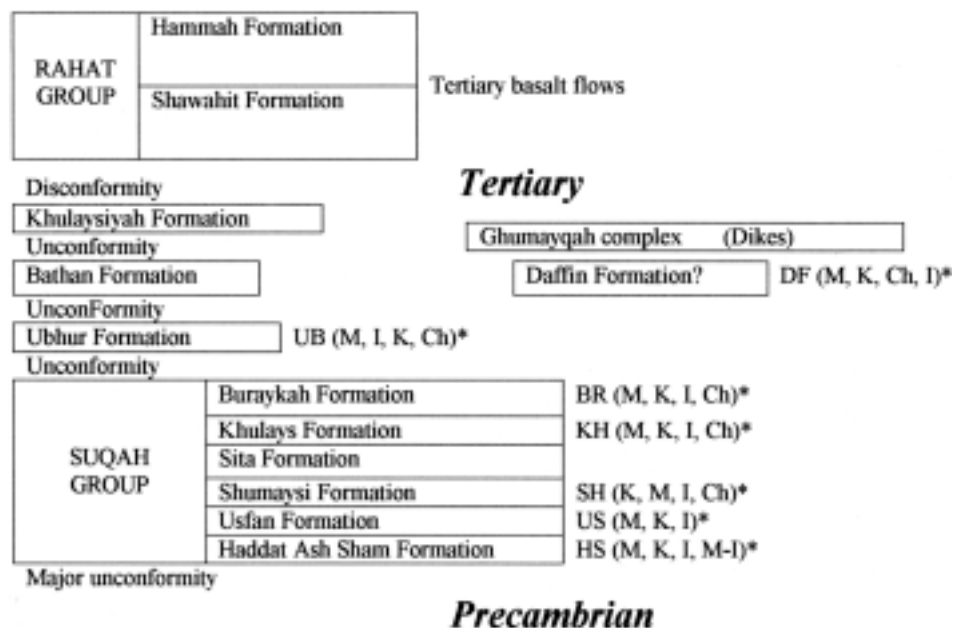
FIG. 2. Tertiary formations in the Makkah and Rabigh quadrangles (Moore & Al-Rehaili, 1989). *Clay minerals are arranged in a descending order: M = Montmorillonite (Ca^{++} and/or Mg^{++} rich variety), K = Kaolinite, I = Illite, Ch = Chlorite and M-I = Mixed layer (Basyoni et al., 2002 and Taj et al., 2002).

(BR), Ubhur (UB) and the youngest Daffin (DF). Any number following these abbreviations indicates its station location. Some authors dealt with the geology of these formations among whom: Brown et al. (1963), Al-Shanti (1966), Karpoff (1975), Spencer and Vincent (1984), Ramsay (1986), Moore and Al- Rehaili (1989) and Zeidan and Banat (1989).

The Tertiary layered rocks of Makkah quadrangle are composed of tilted and faulted strata, which are exposed sporadically, and usually poorly, beneath a cover of flat-lying lavas and Quaternary deposits in the western part of the quadrangle. They were assigned by Brown et al. (1963) to the Shumaysi and Usfan formations. Spencer and Vincent (1984) divided the Shumaysi Formation into the Haddat Ash-Sham, Shumaysi, Khulays and Buraykah formations. These four formations, together with the Usfan Formation, and the Sita Formation of Pallister (1982 & 1986), are grouped into the Suqah group (Fig. 2). It is possible that the Haddat Ash-Sham, Usfan and Shumaysi formations are facies variants and thus chronostratigraphic near-equivalents (Spencer and Vincent, 1984).

Tertiary sedimentary rocks in the western part of the Rabigh quadrangle are best preserved adjacent to where they have been covered by Tertiary basalt flows; elsewhere, they occur in low hills rising above the coastal plain, largely concealed by sand and gravel. The rocks are generally horizontal but have been faulted and consequently attain flexure dips, in places, as much as 40º. They lie unconformably beneath Tertiary lava flows and unconformably overlie, or are faulted against, the Precambrian rocks. They have been assigned to the Usfan, Shumaysi (?), and Daffin formations (Ramsay 1986) .

The studied formations were faulted and tilted, but not folded. They rest unconformably on the Precambrian basement rocks (Fig. 3), and are in turn, overlain by Tertiary to Quaternary basalt lava flows of the Rahat group, which are flat-lying and essentially undeformed (Fig. 4). Their outcrops are discontinuous and form low to medium relief ridges surrounded by the Precambrian crystalline rocks and the Quaternary alluvial and eolian deposits.

Lithologically, all the studied formations consist mainly of siliciclastic material presumably derived from the surrounding Precambrian basement and pre-existing sedimentary rocks. However, the overwhelming clastic sedimentation is temporarily interrupted by limited but persistant marine and lacustrine carbonate units in Usfan Formation, US 9 (Fig. 5) and Daffin Formation, DF 35 (Fig. 6). The sedimentary sequences of the studied formations have a limited extent. The unconformable base of these formations, in some instances, is marked by the occurrence of basal conglomerates. In some cases the beds of these formations are gently dipping to the northeast (Fig. 7). Spencer and Vincent (1984) assigned that the Khulays Formation may be discordantly overlain by the Shumaysi Formation in Fajj Al-Kuraymi at the southeastern end of the Sugah trough. The Buraykah Formation is possibly unconformable on the Khulays Formation (Spencer and Vincent, 1984). However, Moore and Al-Rehaili (1989) considered that the Khulays Formation is conformably overlain by the Buraykah Formation.

Some minor faults, affect different parts of the studied formations, are of the normal type, and trending NE-SW. Dragging took place at the contacts of the fault plane (Fig. 8) indicating the direction of the foot wall. This fault trend is in accordance with the direction of the graben fault system, which had been taken place in post-Oligocene time, in connection with the development of the Red Sea Rift system .

A detailed mineralogical study of the same formations is given by Basyoni *et al.*, (2002) and Taj *et al.*, (2002). The result of their work showed that the relative abundance of the studied clay deposits are of three types. The first, which is the most common, is highly montmorillonitic, the second is made up of a

FIG. 3. Fissile hard ferruginous shale, intercalated by thin bands and pockets of gypsum. This sedimentary sequence is directly impinged on Precambrian basement rocks as indicated by its irregular paleorelief, station: DF 37 (Al-Jafa).

FIG. 4. A general view of fissile olive grey clay with gypsum bands and pockets intercalations. Differential weathering occurs through the hard crumpled sandstone bed overlying the eroded shale. A flat plateau of dark basaltic lava flows (Harrat) topping up the succession

Fɪɢ. 5. A distinctive fossiliferous limestone ledge distinguishing Usfan Formation in the field. The upper part includes black shale and sandstone (Paleocene-lower Eocene). Usfan beds are dipping towards northeast at an angle of 15º-25º, Station : US9, Haddat Ash-Sham locality.
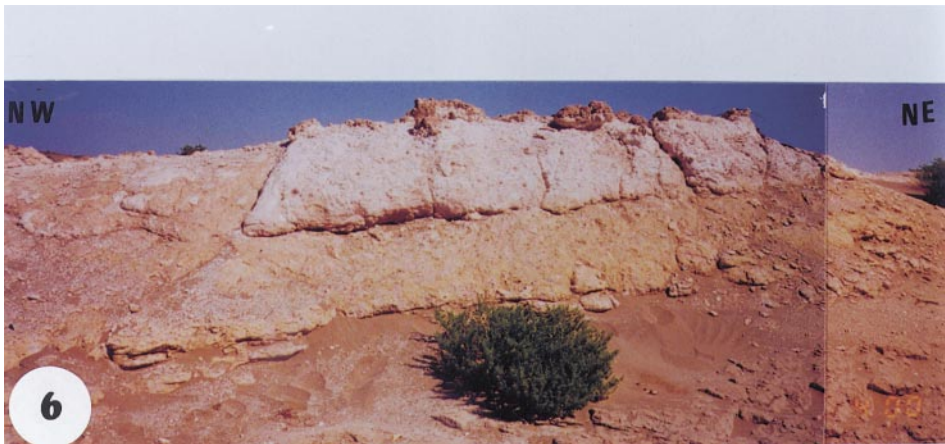
Fɪɢ. 6. Medium relief limestone ridge of Daffin Formation (DF35) extending NW-NE, consists of three parts. The upper one, 1.5 m thick is white, fossiliferous, hard limestone. The middle part, 1m thick is pale yellowish brown, ferruginous sandy limestone. The lower part is greyish pebbly calcareous sandstone (2 ms thick). Precambrian crystalline rocks are out-cropping near this ridge (out of the photo).
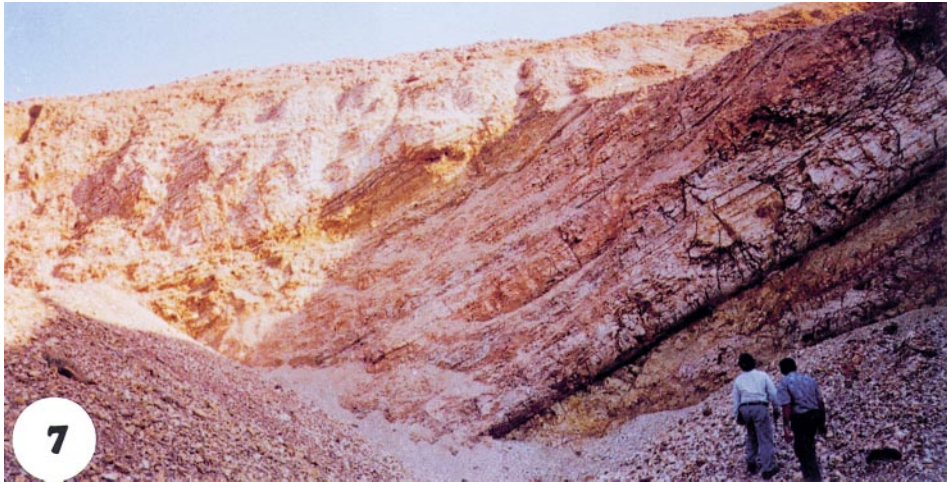
FIG. 7. Well defined angular unconformity between the inclined greyish white clay bed, dipping 20ºNE, and the overlying yellowish white clayey sandstone. Station: SH30, El-khayat quarry, W. Jabal Abu Mukassar.

FIG. 8. Minor fault (F-F) affecting Usfan succession (US8) trending NE-SW. Dragging is observed at the contact of the fault plane, indicating the foot wall direction of the normal fault. Thin bands (reach 25 cm) of clayey sandstone (white) are intercalated the chocolate brown clay deposit.

mixture of montmorillonite followed by kaolinite and illite, and the third is highly kaolinitic with some montmorillonite. They added that kaolinite is generally increased southward in Makkah quadrangle. While chlorite, as minor component shows a northward increase in Rabigh quadrangle. Based on X-ray diffraction analysis of the clay fractions of the studied samples, the identified clay minerals and their abundances are illustrated in Table (1).

TABLE 1. Identified clay minerals and their relative abundance in the clay fractions of the studied samples, (1) Basyoni *et al.,* 2002; (2) Taj *et al.,* 2002.

Formation	Station no.	Sample no.	Montmor- illonite (M)	Kaolinite (K)	Illite (I)	Chlorite (Ch)	Mixed layer (M-I)	Remarks
(1) Haddat Ash Sham	HS10	62	++	+++	+++	–	–	
		63	++++	+++	++	–	–	
		64	+++	+++	++	–	–	
(1) (Usfan)	HS27	92	–	++	–	–	+++++	
	US6	26	+++++	++	+	–	–	
	US7	28	++++	+++	+	+	–	
		30	+++++	++	+	+	–	
	US8	31	+++++	+	+	–	–	
		32	++++	+++	++	–	–	
		33	++++	++	+	–	–	
		34	++	++++	+	–	–	
		36	++	+++++	+	–	–	
		38	+++	++++	++	–	–	
		39	++	++++	++	–	–	
		40	+++++	++	–	–	–	
		41	++++	+++	–	–	–	
		42	+++	+++	++	–	–	
		43	+++++	+	+	–	–	
		44	++	++++	++	–	–	
		45	++++	++	+	–	–	
		46	+++	+++	++	–	–	
		47	+++++	++	+	+	–	
		49	++++	++	++	–	–	
		50	++++	++	++	–	–	
		52	+++	++++	++	–	–	
		53	+++	++++	++	–	–	
		53A	+++	+++	++	–	–	
		54	+++	++++	–	–	–	
		56	+++	++++	–	–	–	
		58	+++	+++	++	–	–	
	US9	59	++	+++	++	–	–	
		61	+++	++++	–	–	–	

R.J. Taj et al.

T<small>ABLE</small> 1. Continued.

Formation	Station no.	Sample no.	Montmor-illonite (M)	Kaolinite (K)	Illite (I)	Chlorite (Ch)	Mixed layer (M-I)	Remarks
(1) Shumaysi	US30	97	++++	++	++	–	–	
		98	++++	+++	++	–	–	
		99	++	++++	++	+	–	
		100	–	+++++	–	–	–	
		101	+++++	+	+	–	–	
		102	–	+++++	–	–	–	
	SH50	132	++++	++	++	–	–	
		133	++++	++	+	–	–	
		134	+++++	++	+	–	–	
		135	++	++++	+	–	–	
(1) Khulays	KH2	KH1	+++++	+	+	–	–	
		KH2	+++++	+	+	–	–	
		KH3	++++++	+	+	–	–	
		KH	++++++	+	+	–	–	Composite sample (KH1,2,3)
	KH3	KHF1	++++++	+	+	–	–	
		KHF2	++++++	+	+	–	–	
		KHF3	+++++	++	++	+	–	
		KHF	++++++	+	+	–	–	Composite sample (KHF1,2,3)
		7	+++++	+	+	–	–	
		8	+++++	++	+	–	–	
		9	++++++	+	+	–	–	
		10	++++++	+	+	–	–	
	KH4	11	++++++	+	+	–	–	
		14	+++++	+	+	+	–	
		17	+++++	+	+	–	–	
	KH5	18	+++++	++	+	–	–	
		19	+++++	++	+	–	–	
		20	+++++	++	+	–	–	
		22	+++++	++	+	+	–	
		23	+++++	++	+	+	–	
		25	+++++	++	–	+	–	
	KH11	65	+++	+++	+++	–	–	
		66	+++	+++	+++	–	–	
		67	++	+++	+++	–	–	
	KH12	68	++	+++	++	++	–	
	KH14	74	++	++++	++	+	–	
		75	++	+++	+++	++	–	

TABLE 1. Continued.

Formation	Station no.	Sample no.	Montmor-illonite (M)	Kaolinite (K)	Illite (I)	Chlorite (Ch)	Mixed layer (M-I)	Remarks
(1) Khulays		76	++	++++	++	++	–	
		77	++++	++	++	–	–	
		78	++	+++++	+	+	–	
		79	++++++	+	+	–	–	
		80	++	++++	++	–	–	
	KH16	82	++++	++	+	+	–	
	KH17	83	+++	++	++	–	–	
		84	++++	++	++	+	–	
	KH20	87	++	++++	++	+	–	
	KH47	126	++++	++	++	–	–	
	KH49	131	+++	++++	–	–	–	
(1) Buraykah	BR13	69	+++	+++	++	+	–	
		70	++++	+++	–	+	–	
		71	++++++	–	+	–	–	
		72	+++++	–	++	++	–	
		73	+++++	++	++	+	–	
(2) Ubhur	UB1	UB1	+++++	+	++	–	–	Grayish white clay
		UB3	+++++	+	+	–	–	Contact between reddish & white clay
		UB4	+++++	+	++	+	–	Hard fissile sandy clay
	UB2	UB129	+++	+++	+++	–	–	Thin greenish grey clay band between massive gypsum & selenite
		UB130	++++	+++	++	–	–	Bottom of the quarry
	UB3	UB89A	++++	++	++	+	–	Core of spheroids
		UB90A	++++	++	++	+	–	Core of spheroids
		UB90B	++++	++	++	–	–	Spalls of spheroids
	UB4	UB91A	+++++	–	++	–	–	Core of spheroids
		UB91B	++++++	–	–	–	–	Spalls of spheroids
(1) Daffin	DF37	114	+++	+++	++	–	–	
	DF38	115	+++	+++	++	–	–	
	DF40	116	+++	++	–	+++	–	Swelling chlorite
	DF41	117	++	++	++	++	–	
		118	++	+++	++	++	–	
	DF42	119	++	+++	++	++	–	

TABLE 1. Continued.

Formation	Station no.	Sample no.	Montmor- illonite (M)	Kaolinite (K)	Illite (I)	Chlorite (Ch)	Mixed layer (M-I)	Remarks
(1) Daffin	DF43	121	–	+++	++	+++	–	
	DF44	122	+++	+++	++	++	–	Core of spheroids
	DF45	123A	++++	++	++	–	–	Spalls of
		123B	+++	++	++	++	–	spheroids
	DF46	125	+++	++	–	+++	–	Swelling chlorite
(1) Haddat Ash Sham	31	103 (36)*	–	+++++	+	–	–	
		104 (45)*	+++	+++	++	+	–	
	32	105 (32)*	+++++	++	+	+	–	
	33	106 (45)*	++++	++	++	+	–	
		107 (70)*	+++++	++	+	–	–	
		108 (120)*	++	+++	++	–	–	
Sub- surface samples	34	109 (90)*	–	+++++	–	–	++	
		110 (90)*	++++	+++	++	–	–	
		111 (120)*	++++	++	+	–	–	
			++++	++	+	–	–	

Symbols for approximate percentage contents are ++++++: more than 90; +++++: 70-90; ++++: 50-70; +++: 30-50; ++:10-30; and + less than 10; –: not recorded.
*Depth in meter.

The present paper is extracted from the final report for King Abdulaziz University Sponsored research, Project No. 203/419 submitted by the same authors (Taj *et al.*, 2001a).

Chemical Composition

Complete chemical analyses of the major oxides and some trace elements (Li, B, V, Cr, Co, Ni, Cu, Zn, Sr, Mo & Pb) were performed on 77 clayey samples from the studied seven formations, among them 4 samples were raised from three boreholes representing the Haddat Ash Sham sub-surface samples (Tables 2-7). Ga & Rb were analysed in 47 clayey samples (Table 7) from the whole analysed ones.

TABLE 2. Major and some trace constituents of bulk samples from Haddat Ash Sham (HS) and Usfan Formations.

Formation		HS		US											US9
Station	D.L.	HS10		US8											
Sample no.		62	63	31	32	33	34	39	40	41	42	43	46	56
SiO_2%	1.00	58.0	53.3	55.5	48.8	54.5	46.7	51.6	51.6	57.6	53.6	62.4	58.2	60.1
Al_2O_3	1.00	12.5	20.1	17.8	24.9	25.3	25.2	17.6	21.6	19.2	20.6	15.4	19.3	19.9
Fe_2O_3*	1.00	6.6	6.4	5.7	10.4	3.1	11.2	14.5	6.8	6.1	8.7	4.2	4.6	1.1
CaO	1.00	2.1	<1.0	1.3	<1.0	1.2	<1.0	1.5	<1.0	<1.0	<1.0	1.1	1.3	<1.0
MgO	1.00	1.2	1.1	1.7	1.1	<1.0	1.3	1.0	1.3	1.2	1.3	1.4	1.3	1.3
K_2O	0.50	2.3	0.7	<0.5	1.0	1.0	1.1	1.0	<0.5	<0.5	0.8	<0.5	<0.5	1.5
MnO	0.01	0.01	0.01	0.02	0.23	0.02	0.03	0.20	0.02	0.01	0.02	0.01	0.01	0.05
TiO_2	0.01	0.67	0.97	0.90	1.15	1.25	1.10	1.01	1.21	1.13	1.16	0.79	1.04	1.58
P_2O_5	0.01	0.113	0.182	0.064	0.169	0.161	0.177	0.551	0.099	0.052	0.108	0.055	0.107	0.076
Na_2O	0.05	0.30	1.48	0.097	0.82	1.00	0.82	1.43	0.82	1.03	0.90	0.85	0.57	0.62
SO_3	0.05	<0.05	<0.05	<0.05	<0.05	<0.05	<0.05	<0.05	<0.05	<0.05	<0.05	<0.05	<0.05	<0.05
L.O.I.	0.05	15.37	13.90	15.29	11.22	11.96	11.25	9.49	13.18	12.08	12.33	12.99	13.26	12.12
Total		89.21	99.2	99.7	100.9	100.5	100.93	99.93	100.16	99.95	100.56	99.75	100.24	99.10
Li (ppm)	10	10	23	10	20	12	23	12	20	15	19	<10	15	36
B	10	33	30	<10	13	<10	19	18	19	<10	18	<10	<10	31
V	10	138	209	217	200	182	211	320	187	171	200	199	227	140
Cr	10	64	221	85	33	62	37	38	93	97	84	64	104	110
Co	5	24	10	26	104	11	24	37	19	17	21	17	19	26
Ni	10	<10	<10	12	<10	<10	<10	<10	11	40	26	36	42	56
Cu	5	13	23	56	112	28	54	79	117	58	118	67	91	122
Zn	5	55	92	83	119	33	122	117	85	100	128	85	74	122
Sr	5	312	300	176	124	597	114	236	−161	151	148	135	257	96
Mo	5	<5	<5	<5	<5	<5	5	7	<5	<5	<5	<5	<5	<5
Pb	10	14	<10	<10	<10	<10	10	14	11	<10	16	<10	<10	20

*Total iron as Fe_2O_3
D.L. Detection Limit

R.J. Taj et al.

TABLE 3. Major and some trace constituents of bulk samples from Shumaysi (SH) and Buraykah Formations.

Formation		HS										Br		
Station	D.L.	HS30						SH50				BR13		
Sample no.		97	98	99	100	101	102	132	133	134	135	69	70	73
SiO_2%	1.00	58.4	68.3	48.4	61.6	62.4	44.9	45.24	54	62.62	43.70	49.9	47.6	61.0
Al_2O_3	1.00	16.8	14.3	18.9	13.6	13.7	25.9	22.40	14.74	17.60	26.60	17.5	15.3	12.9
Fe_2O_3*	1.00	5.7	1.6	11.9	6.0	5.4	11.2	12.48	6.63	8	12.43	8.7	15.5	2.7
CaO	1.00	1.0	<1.0	1.0	<1.0	1.0	<1.0	1.10	3.90	0.50	0.60	2.1	1.4	2.1
MgO	1.00	1.2	<1.0	1.3	1.5	1.4	<1.0	1.42	4.50	0.40	1.00	2.4	2.4	2.6
K_2O	0.50	<0.05	<0.5	<0.5	<0.5	<0.5	<0.5	0.65	1.80	0.20	0.70	0.5	0.5	1.0
MnO	0.01	0.01	0.01	0.09	0.02	0.01	0.07	0.10	0.10	0.10	0.10	0.06	0.15	0.07
TiO_2	0.01	0.95	0.81	0.97	0.72	0.73	1.16	1.35	0.87	1.00	1.37	1.37	1.43	0.73
P_2O_5	0.01	0.094	0.037	0.169	0.057	0.073	0.197	0.26	0.23	0.22	0.27	0.228	0.207	0.122
Na_2O	0.05	0.62	0.43	0.51	0.84	0.74	0.45	1.47	2.51	0.40	0.31	1.20	1.28	2.52
SO_3	0.05	<0.05	<0.05	<0.05	<0.05	<0.05	<0.05	<0.05	0.05	1.36	<0.05	<0.05	<0.05	<0.05
L.O.I.	0.05	13.89	11.69	15.43	13.47	13.54	13.65	11.27	10.42	8.79	12.72	15.83	13.83	11.00
Total		99.30	99.73	99.22	99.36	99.47	100.08	98.79	99.75	101.09	99.75	99.84	99.65	99.79
Li (ppm)	10	<10	13	15	<10	<10	23	<10	35	13	21	16	13	<10
B	10	11	11	24	13	13	51	26	76	44	40	66	69	24
V	10	197	123	223	146	160	222	123	148	169	221	189	221	141
Cr	10	110	91	99	71	73	98	88	139	97	133	117	105	49
Co	5	12	<5	31	24	18	29	6	20	18	27	32	40	16
Ni	10	53	51	63	81	48	63	38	58	70	98	44	13	10
Cu	5	59	43	88	90	51	87	48	43	52	85	57	72	37
Zn	5	105	53	161	122	98	106	51	119	84	127	115	122	78
Sr	5	104	92	99	102	105	163	99	188	190	136	161	185	235
Mo	5	5	<5	6	<5	<5	6	<5	5	<5	5	<5	6	<5
Pb	10	<10	<10	13	16	15	27	<10	10	13	15	<10	11	10

*Total iron as Fe_2O_3
D.L. Detection Limit

T<small>ABLE</small> 4. Major and some trace constituents of bulk samples from Khulays Formation (KH).

Formation		KH											
Station	D.L.	KH_2			KH_3							KH_4	
Sample no.		1	2	3	F1	F2	P3	7	8	9	10	13	14
SiO_2%	1.00	54.7	57.3	51.7	75.7	51.6	51.6	45.0	49.2	65.6	51.1	51.0	51.1
Al_2O_3	1.00	16.2	17.8	16.1	7.8	19.0	19.0	18.0	19.9	14.2	19.0	14.1	16.7
Fe_2O_3*	1.00	6.7	6.2	6.3	3.7	10.7	12.5	11.7	9.3	4.1	10.0	8.1	8.6
CaO	1.00	1.3	1.0	1.7	1.1	1.2	1.0	5.3	2.2	1.1	1.0	4.6	1.2
MgO	1.00	2.1	1.4	*2.1	1.1	1.4	1.4	1.7	1.8	1.2	1.3	1.4	1.8
K_2O	0.50	<0.5	0.5	<0.5	0.6	0.6	1.6	<0.5	<0.5	0.5	0.5	<0.5	<0.5
MnO	0.01	0.02	0.01	0.01	0.07	0.04	0.04	0.05	0.03	0.02	0.02	0.02	0.02
TiO_2	0.01	1.14	1.11	1.10	0.62	1.27	1.28	1.14	1.27	0.87	1.25	0.87	0.96
P_2O_5	0.01	0.125	0.061	0.297	0.076	0.289	0.205	0.551	0.215	0.051	0.101	0.061	0.158
Na_2O	0.05	1.80	0.95	2.10	1.44	0.81	0.77	0.80	0.88	0.81	0.86	1.17	1.51
SO_3	0.05	<0.05	<0.05	<0.05	<0.05	<0.05	<0.05	<0.05	<0.05	<0.05	<0.05	<0.05	<0.05
L.O.I.	0.05	15.22	13.70	17.50	7.35	13.22	12.40	15.83	15.54	11.22	14.62	17.93	17.19
Total		99.86	100.08	99.46	99.64	100.18	100.85	100.62	100.89	99.92	99.8	99.80	99.76
Li (ppm)	10	<10	12	<10	<10	15	15	13	14	<10	14	<10	<10
B	10	34	24	30	13	37	34	46	47	24	40	43	51
V	10	167	204	161	117	194	246	241	200	201	204	169	202
Cr	10	91	114	87	110	85	77	84	102	70	94	79	86
Co	5	10	16	10	10	29	32	30	27	17	23	40	42
Ni	10	32	51	17	<10	<10	11	22	18	16	12	37	20
Cu	5	44	52	41	21	42	59	111	80	295	46	37	35
Zn	5	108	84	84	43	109	119	1.00	108	76	105	71	81
Sr	5	177	154	214	114	153	152	148	175	126	146	163	149
Mo	5	<5	<5	<5	<5	<5	<5	<5	<5	<5	<5	<5	<5
Pb	10	<10	<10	<10	<10	<10	<10	<10	<10	<10	<10	<10	<10

*Total iron as Fe_2O_3
D.L. Detection Limit

TABLE 4. Continued.

Formation		KH												
Station	D.L.	KH5			KH11			KH14			KH17	KH20	KH48		KH49
Sample no.		19	22	25	65	66	67	74	76	79	83	87	127	128	131
SiO_2%	1.00	53.6	80.2	51.0	53.5	49.7	50.7	48.9	57.9	61.1	48.3	52.1	89.21	63.34	64.26
Al_2O_3	1.00	16.2	7.3	21.7	17.6	17.6	17.5	18.3	16.3	12.8	14.2	20.3	4.20	13.43	15.60
Fe_2O_3*	1.00	12.8	2.2	8.0	6.5	7.7	7.2	12.0	7.0	4.5	6.8	8.8	1.84	7.0	2.06
CaO	1.00	1.0	<1.0	<1.0	1.2	1.3	1.1	1.0	<1.0	1.1	6.3	<1.0	<1.0	1.23	<1.0
MgO	1.00	<1.0	<1.0	1.0	2.0	2.2	2.0	1.7	1.4	1.8	2.0	1.0	1.0	1.64	<1.0
K_2O	0.50	<0.05	<0.5	<0.5	<0.5	<0.5	<0.5	<0.5	<0.5	<0.5	0.9	0.5	<0.50	0.50	0.56
MnO	0.01	0.04	0.02	0.02	0.04	0.03	0.02	0.05	0.03	0.01	0.07	0.03	0.10	0.10	0.10
TiO_2	0.01	2.06	0.81	1.40	1.14	1.37	1.23	1.51	1.47	0.80	1.02	1.22	0.23	0.69	0.50
P_2O_5	0.01	0.243	0.0247	0.117	0.169	0.305	0.180	0.217	0.097	0.046	0.171	0.236	0.10	0.20	0.27
Na_2O	0.05	0.38	0.23	0.74	1.73	1.70	1.94	1.13	0.97	0.86	1.86	0.72	0.24	0.60	0.56
SO_3	0.05	<0.05	<0.05	<0.05	<0.05	<0.05	<0.05	<0.05	<0.05	<0.05	<0.05	<0.05	<0.05	<0.05	<0.05
L.O.I.	0.05	12.23	6.44	15.05	15.66	16.89	17.08	13.90	12.37	15.76	17.79	13.93	3.31	10.56	13.80
Total		100.10	99.35	100.58	100.09	99.35	99.5	99.26	99.10	99.33	99.46	99.89	101.78	99.24	99.66
Li (ppm)	10	15	<10	20	12	16	12	13	10	<10	17	39	<10	<10	17
B	10	31	17	21	59	63	60	70	52	30	57	78	25	28	56
V	10	227	63	373	181	185	176	227	207	239	180	195	79	140	223
Cr	10	143	71	142	100	102	98	116	115	94	99	114	60	250	146
Co	5	42	19	29	15	36	13	46	13	31	15	18	10	31	26
Ni	10	12	13	32	31	37	46	13	30	47	18	<10	58	76	78
Cu	5	46	26	82	54	49	44	37	70	47	50	28	23	106	121
Zn	5	133	56	153	116	89	112	104	129	73	95	98	35	233	112
Sr	5	149	108	204	159	147	136	147	125	148	178	199	61	98	182
Mo	5	<5	<5	7	<5	<5	<5	5	<5	<5	5	<5	<5	<5	<5
Pb	10	16	<10	19	<10	<10	<10	13	12	<10	<10	25	<10	13	14

*Total iron as Fe_2O_3
D.L. Detection Limit

TABLE 5. Major and some trace constituents of bulk samples from Ubhur Formation (UB) and boreholes (HS).

Formation		UB								HS (subsurface samples)			
Station	D.L.	UB22		UB23				UB24		St. 31	St. 33	St. 34	
Sample no.		129	130	89A	89B	90A	90B	91A	91B	103	106	109	110
SiO_2%	1.00	50.20	63.74	63.6	62.6	59.5	62.1	77.4	76.4	48.4	52.4	50.1	56.6
Al_2O_3	1.00	18.46	13.63	12.3	13.3	13.4	13.1	7.4	6.9	22.9	19.6	20.1	20.0
Fe_2O_3*	1.00	6.50	7.40	5.9	5.6	5.6	6.3	2.9	2.8	12.1	8.3	8.8	7.7
CaO	1.00	<1.0	1.10	1.6	1.6	2.8	2.0	1.2	1.3	<1.0	2.1	1.2	<1.0
MgO	1.00	4.00	1.33	2.1	2.3	2.4	2.5	1.5	1.4	<1.0	2.0	1.4	1.1
K_2O	0.50	2.34	0.71	1.8	1.8	1.5	1.6	0.9	0.8	0.5	1.5	<0.5	0.5
MnO	0.01	0.12	0.1	0.05	0.07	0.05	0.07	0.07	0.04	0.02	0.10	0.03	0.10
TiO_2	0.01	0.91	0.68	0.79	0.83	0.85	0.85	0.50	0.53	1.16	0.98	0.87	1.19
P_2O_5	0.01	0.23	0.19	0.155	0.158	0.160	0.153	0.030	0.026	0.173	0.144	0.091	0.087
Na_2O	0.05	1.4	0.6	2.00	1.86	1.86	1.74	1.03	0.97	0.50	0.80	0.27	0.41
SO_3	0.05	<0.05	<0.05	<0.05	<0.05	<0.05	<0.05	<0.05	<0.05	<0.05	<0.05	<0.05	<0.05
L.O.I.	0.05	11.69	10.3	9.19	9.46	12.34	9.07	6.79*	8.36	12.68	12.11	15.76	11.33
Total		99.5	99.49	99.53	99.63	99.62	99.53	99.77	99.58	99.46	100.18	99.17	100.07
Li (ppm)	10	116	<10	21	24	24	26	<10	<10	16	15	15	18
B	10	157	32	58	5Z	65	65	25	21	42	15	10	12
V	10	162	134	123	135	142	153	75	67	203	183	204	144
Cr	10	113	168	111	123	118	123	53	53	117	109	84	77
Co	5	2 9	56	18	16	17	15	6	6	16	25	19	19
Ni	10	67	130	<10	48	38	48	28	38	52	41	35	40
Cu	5	80	80	31	35	43	67	17	18	58	41	83	32
Zn	5	129	167	97	94	101	124	76	80	104	100	77	108
Sr	5	226	87	186	188	167	162	132	125	192	149	166	129
Mo	5	6	<5	<5	<5	<5	5	<5	<5	7	5	5	129
Pb	10	10	<10	1.5	16	<10	13	10	16	21	24	16	14

*Total iron as Fe_2O_3
D.L. Detection Limit

R.J. Taj et al.

TABLE 6. Major and some trace constituents of bulk samples from Daffin Formation (DF).

Formation		DF												
Station	D.L.	DF36	DF37	DF38	DF40	DF41		DF42	DF43	DF44	DF45		DF46	DF47
Sample no.		113#	114	115	116	117	118	119	121	122	123A	123B	125	126
SiO$_2$%	1.00	3.50	48.50	58.32	55.00	47.00	49.00	52.70	52.20	51.50	56.40	56.65	56.86	61.32
Al$_2$O$_3$	1.00	0.40	18.20	17.40	16.80	17.00	14.20	17.00	18.04	17.00	17.00	16.50	16.10	14.00
Fe$_2$O$_3$*	1.00	0.21	9.15	9.30	5.50	8.20	12.17	8.30	8.87	8.96	7.58	7.40	9.56	9.80
CaO	1.00	32.55	2.00	1.80	2.00	4.50	3.20	2.00	1.62	1.84	2.10	2.20	3.34	0.60
MgO	1.00	0.25	2.84	0.80	4.00	3.20	2.63	4.50	4.30	3.81	2.60	2.84	2.20	1.42
K$_2$O	0.50	0.04	1.60	1.30	0.60	1.60	1.72	2.00	2.11	2.10	1.60	1.70	0.75	0.70
MnO	0.01	0.01	0.01	0.04	0.10	0.10	0.10	0.10	0.10	0.10	0.15	0.15	0.13	0.10
TiO$_2$	0.01	0.10	1.04	1.32	0.80	1.00	1.30	1.10	1.13	1.10	1.22	1.19	1.07	1.77
P$_2$O$_5$	0.01	0.27	0.10	0.10	0.10	0.50	0.20	0.10	0.10	0.10	0.20	0.30	0.90	0.10
Na$_2$O	0.05	0.10	1.20	1.50	2.00	2.10	3.00	1.50	1.60	2.52	2.52	2.50	1.70	1.12
SO$_3$	0.05	43.90	<0.05	<0.05	<0.05	<0.05	<0.05	<0.05	<0.05	<0.05	<0.05	<0.05	<0.05	<0.05
L.O.I.	0.05	19.84	15.21	10.01	12.60	14.55	12.23	10.02	9.77	10.72	8.34	8.38	7.00	8.85
Total		101.17	99.74	89.85	99.50	99.75	99.76	99.62	99.85	99.65	89.71	99.81	99.61	99.78
Li (ppm)	10	<10	94	<10	28	31	22	37	31	50	35	37	14	<10
B	10	15	102	60	46	66	62	95	98	109	61	60	48	74
V	10	<10	179	186	147	167	146	161	168	167	201	171	194	185
Cr	10	26	120	114	107	105	144	172	154	116	131	134	66	250
Co	5	<5	15	12	26	22	20	28	28	24	48	36	29	30
Ni	10	<10	77	50	80	58	38	103	83	70	59	64	30	79
Cu	5	6	62	28	46	43	28	52	44	25	70	92	40	41
Zn	5	11	83	98	102	84	78	98	88	89	117	91	132	95
Sr	5	590	222	166	228	371	389	202	203	262	238	239	190	113
Mo	5	<5	<5	5	5	5	5	<5	<5	262	238	5	190	5
Pb	10	<10	10	10	<10	<10	13	10	10	10	26	19	10	10

*Total iron as Fe$_2$O$_3$ #Gypsum Sample
D.L. Detection Limit

TABLE 7. Ga & Rb contents (ppm) in selected samples from the studied formations.

Serial	Sample no.	Station	Formation	Ga (ppm)	Rb (ppm
				D.L.	5
1	62	HS10	Haddat As Sham	15.8	36.0
2	63			28.3	14.0
3	32	US8	Usfan	29.3	11.0
4	33			40.0	6.0
5	39			20.5	14.0
6	41			24.9	8.0
7	43			22.6	11.0
8	98	SH30	Shumaysi	23.8	5.0
9	99			21.3	11.0
10	100			20.5	8.0
11	101			20.7	8.0
12	102			28.5	14.0
13	132	SH50		15.0	45.0
14	133			16.0	45.0
15	134			15.0	11.0
16	135			24.0	26.0
17	70	BR13	Burayka	17.1	7.0
18	73			16.7	8.0
19	KHF1	KH3	Khulays	12.5	5.0
20	KHF3			21.6	7.0
21	10			22.8	9.0
22	14	KH4		22.0	8.0
23	25	KH5		29.6	9.0
24	79	KH14		20.0	5.0
25	127	KH48		6.0	5.0
26	128			13.0	20.0
27	131	KH49		19.0	24.0
28	129	UB22	Ubhur	18.0	71.0
29	130			13.0	21.0
30	90A	UB23		17.6	12.0
31	90B			17.2	14.0
32	91A	UB24	Boreholes*	13.1	9.0
33	106	BH33		24.1	17.0
34	110	BH34		25.5	9.0

TABLE 7. Continued.

Serial	Sample no.	Station	Formation	Ga (ppm)	Rb (ppm
				D.L.	5
35	113	**DF36**		<5	5
36	114	**DF37**		17.0	46.0
37	115	**DF38**		17.0	32.0
38	116	**DF40**		15.0	16.0
39	117	**DF41**		18.0	41.0
40	118			16.0	39.0
41	119	**DF42**	Usfan	16.0	46.0
42	121	**DF43**		17.0	50.0
43	122	**DF44**		17.0	40.0
44	123	**DF45**		18.0	30.0
45	123B			20.0	31.0
46	125	**DF46**		15.0	16.0
47	126	**DF47**		14.0	15.0

D.L. Detection Limit

Major Constituents

Alumina and Silica

Alumina and silica are known to be the most important major oxides constituting the clay minerals. They are inversely related where an increase in one of them is accompanied by a decrease in the other as shown in samples of all formations (Fig. 9, A-E and Tables 2-6).

Silica content in the analysed clayey samples ranges between 43.70% and 89.21% (Tables 3 & 4 cont.). In some of the analyzed samples, the amount of SiO_2 is higher than the theoretical value required for Al_2O_3 to make aluminosilicate clay minerals. The remainder amount constitutes the detrital silty to sandy quartz grains, which are commonly observed in the samples either by the naked eye, or by using a hand lens or through the mineralogical investigations. Generally, the highest SiO_2 percents were recorded in several samples of Khulays and Ubhur formations, those samples are mainly of sandy nature. On the other hand, the lower values of SiO_2 were recorded in some pure clay samples of the different studied formations.

Alumina content ranges between 4.20% and 26.60% (Tables 4, cont. & 3). Generally, the samples having the lowest and highest Al_2O_3% are themselves showing the highest and lowest SiO_2% confirming the inverse relation between
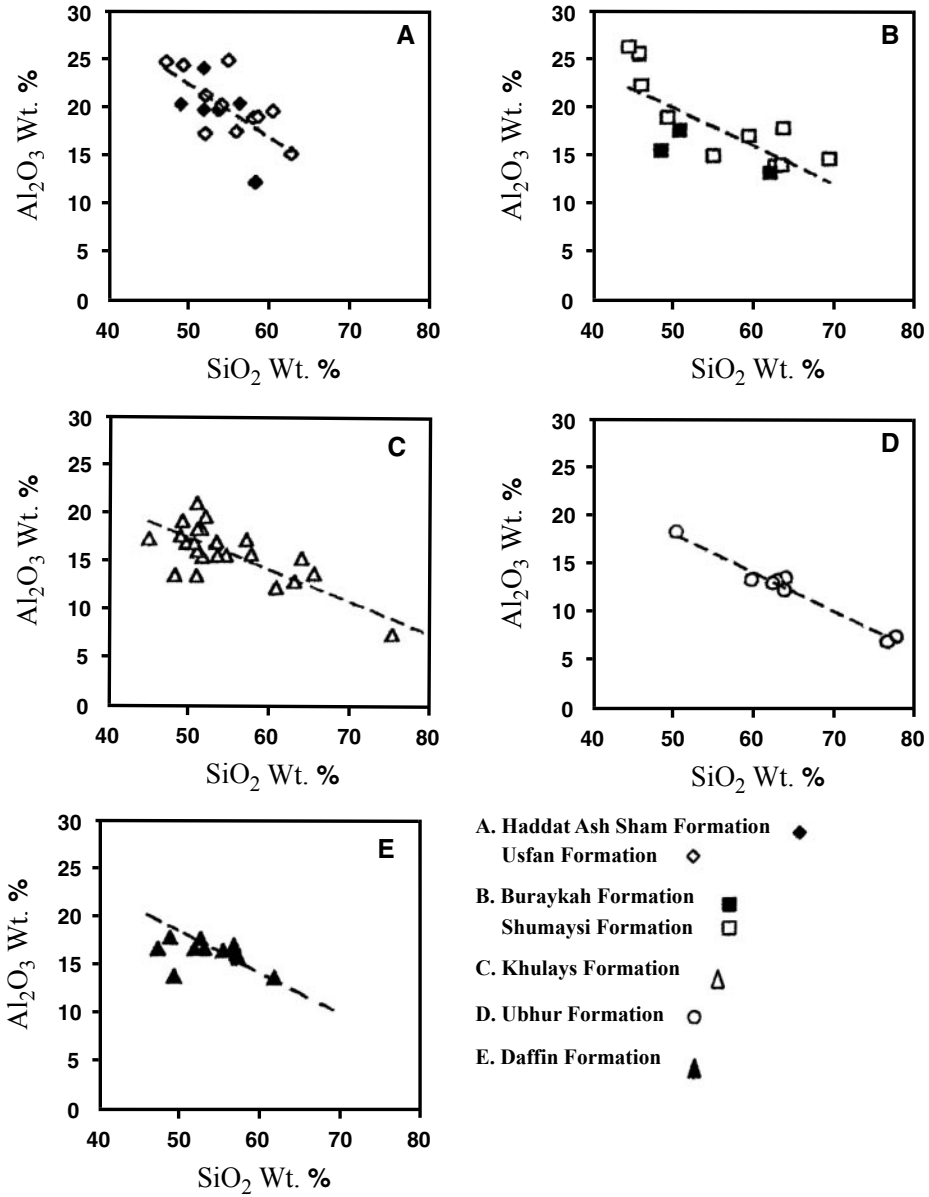
FIG. 9. Binary relations diagrams (A-E) between SiO_2 and Al_2O_3 wt.%.

Al_2O_3 and SiO_2. The highest Al_2O_3 percents are recorded in samples having the highest kaolinite content and in pure clay samples composed essentially or totally of clay minerals (Table 1). Generally the lowest alumina content values are recorded in some samples of Khulays and Ubhur formations, which are mostly of argillaceous nature and not proper clay deposits. Silty and sandy clay samples of the other formations show also low Al_2O_3 content.

Total Iron (Fe_2O_3) and MnO

Total iron expressed as Fe_2O_3 ranges from 1.1% to 15.5% (Tables 2 & 3) in the investigated clay samples. The total iron content of most of the analyzed samples lies in the middle of this range. Some samples are completely stained with iron oxides giving them the reddish brown or chocolate colors. This is due to the presence of iron-bearing minerals as goethite which has been also revealed by thermal analyses (Basyoni *et al*., 2002).

MnO occurs in minor amounts ranging from 0.01% to 0.23% (Table 2). Its content in the majority of the analyzed samples lies near the lower limit of this range. However, samples having relatively high MnO content contain also high Fe_2O_3. This confirms the proportional relation between the two oxides (Fig. 10, A-E). The visible occurrences of the tubercular and dendrite forms of Mn-minerals in several localities of the studied formations reflect the increase of MnO% in the corresponding samples. The presence of most manganese minerals, in thin fractures, near the surface is pervasive and probably represents the earliest stage of supergene alteration (Sorem & Gunn, 1967 and Tosson & Saad 1974).

CaO & MgO

Both oxides occur in relatively smaller amounts as compared with the foregoing oxides. CaO ranges from <1.0% to 6.3% (Table 2 & 4 cont.) in the analyzed clayey samples. The low values are recorded mostly in Usfan and Shumaysi samples, while the higher values are recorded in Khulays and Daffin samples. Similarly, MgO ranges from <1.0% to 4.5% (Tables 3 & 6). Usfan and most Shumaysi samples show the lowest MgO content, while Buraykah, Khulays, Ubhur and Daffin samples show higher content of MgO.

The CaO and MgO contents increase or decrease according to the relative abundance of calcite, gypsum, montmorillonite and chlorite. Ca^{++} and /or Mg^{++} are readily accommodated in montmorillonite, which is mineralogically detected in most of the analyzed clay samples especially those of Khulays and Buraykah formations that have higher contents of both oxides. Chlorite (Table 1) could be also considered as a contributor for MgO where it is recorded in the three analyzed Buraykah samples that contain the highest MgO content (Table
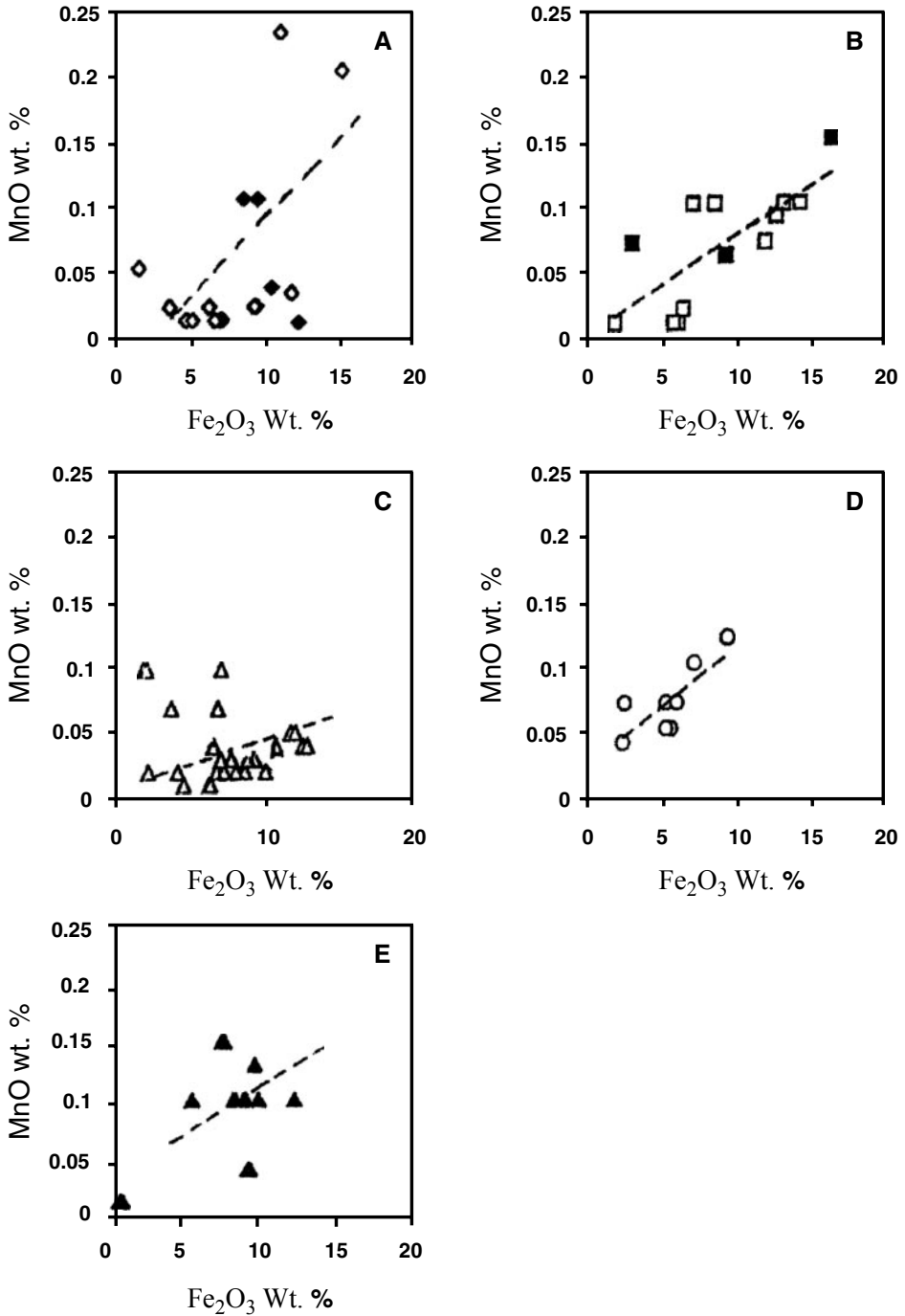
F<small>IG</small>. 10. Binary relations diagrams (A-E) between Fe$_2$O$_3$ and MnO wt.% (Symbols as in Fig. 9).

3). The lowest CaO and MgO contents recorded in Usfan and Shumaysi samples are due to their sandy and ferruginous nature, which is identified by a higher kaolinite content than montmorillonite (Table 1). Gypsum and calcite, which often fill thin veinlets, could be considered as minor contributors for CaO.

K_2O & Na_2O

The analyzed clayey samples generally have low K_2O & Na_2O contents. K_2O ranges from < 0.5%, in many samples of Shumaysi, Usfan and Khulays formations (Tables 2-4), to 2.3%-2.34% in two samples of Haddat Ash-Sham and Ubhur formations, respectively (Tables 2 &5). The concentration of K_2O in most samples seems to follow the distribution of the illite. The highest illite content recorded is about 40% illite (Samples 62 & 129, Table 1) contains the highest K_2O content. Most of the analyzed Ubhur Formation samples have an average of about 1.5% K_2O and about 20% illite. Potassic feldspar minerals share illite as potassium contributors.

Na_2O content ranges from 0.097% to 3.00% (Tables 2 & 6). It is attributed to the presence of water soluble NaCl salt and sodic plagioclase feldspar. The lowest Na_2O content which was recorded in one of the samples contain a high montmorillonite percentage (Sample 31, Tables 1 &2) may indicate the non contribution of Na^+ as exchangeable cation in the montmorillonite structure. However, the results of mineralogical analysis confirms that the exchangeable cations of montmorillonite are Ca^{++} (Basyoni *et al.*, 2002).

TiO_2

TiO_2 ranges from 0.50% to 2.06% (Tables 5 & 4) in all studied samples. Its average content in the samples of the different formations is as follows: Haddat Ash Sham (0.82%), Usfan (1.12%), Shumaysi (0.85%), Buraykah (1.18%), Khulays (1.10%), Ubhur (0.74%) and Daffin (1.08%). The TiO_2 content is mainly due to the expected titanium-bearing heavy minerals, *e.g.* rutile, ilmenite and sphene. Minor titanium amount can readily replace Al^{+3} in the kaolinite lattice (El Askary and El Mahdy, 1976). Keith and Degens (1959) concluded that the fresh water muds contain about 1-3.5 wt% Ti (1.66-5.8 wt% TiO_2), while most marine muds contain less than 0.7 wt% Ti (1.16 wt% TiO_2). Accordingly, the aforementioned averages of TiO_2 wt% could suggest marine to transitional depositional environments for the studied mudrocks of the seven formations.

SO_3

SO_3 is recorded in scarce amount, being <0.05% (below the detection limit of the apparatus used in the analysis) in all the analyzed samples (Tables 2-6). Its

content is most probably attributed to the presence of gypsum, which occasionally is associated with the studied clay rocks, either as strings or minute pockets.

L.O.I.

Loss on ignition values show considerable variation in the analyzed clayey samples either in those from different localities or in the samples of the same locality. It ranges from 3.31% to 17.93% (Table 4, cont.). The lowest L.O.I. values are recorded in the silty and sandy clay samples which contain high silica content. Accordingly, there is an inverse relation between L.O.I. and SiO_2 contents in the majority of samples as indicated in figure (11, A-E). The L.O.I. wt% corresponds essentially to the hygroscopic and crystalline water of the clay mineral suite, and in few samples, to the water of crystallization of gypsum and goethite which is recorded by thermal analysis technique (Basyoni *et al*., 2002). It could be also, to a lesser extent, due to the expelled CO_2 gas of the less commonly occurring carbonates in the studied samples.

P_2O_5

The P_2O_5 wt% in the analysed samples varies from 0.026 wt% to 0.90 wt% (Tables 5 & 6). Phosphorous is most probably adsorbed on the different clay minerals or present as hydrated calcium phosphate. It is evident that, in most of the analysed samples, there is a characteristic decrease in P_2O_5 with increase in the CaO contents. The subordinate amount of P_2O_5 could indicate that the studied clay deposits in the different formations are probably originated from the effect of weathering solutions, which are geochemically characterized by a higher content of phosphorus than those derived from volcanic processes (Harder, 1964).

Trace Elements

The following eleven trace elements were determined: Li, B, V, Cr, Co, Ni, Cu, Zn, Sr, Mo, and Pb in the same 77 selected samples, which cover all the studied formations. Two more trace elements Ga and Rb were also determined in 47 samples selected from the different formations. Some chemical data are graphically treated and discussed in conjunction with the depositional environments.

Several geochemical studies based on trace elements are performed as clay minerals contain major part of traces due to their reactivity, variability of structure and the very small grain size (El Sherbini, 1995). Clay minerals and trace elements seem to be regulated and stabilized by depositional environment (Saad, 1996).
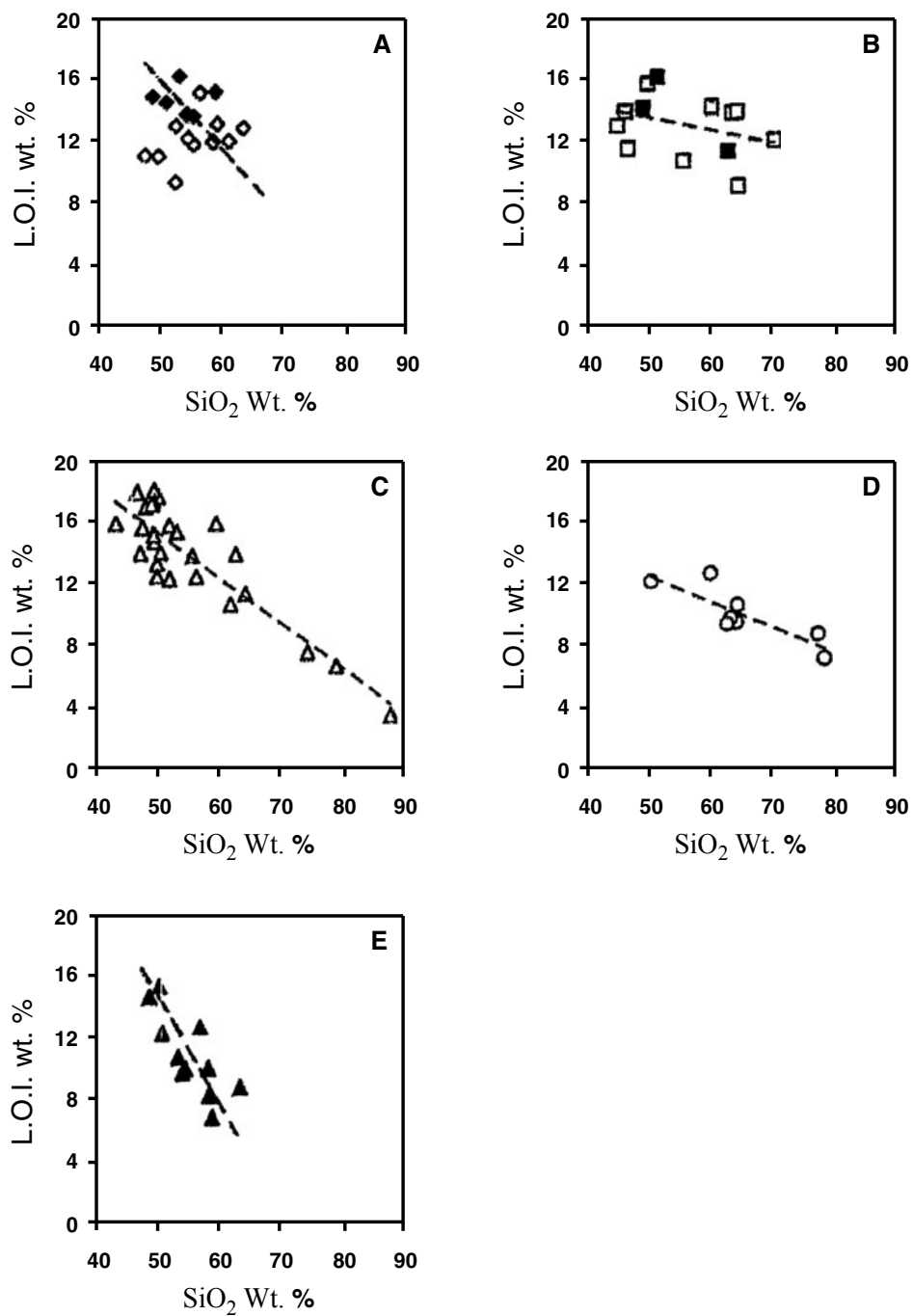
FIG. 11. Binary relations diagrams (A-E) showing the inverse relation between SiO_2 and L.O.I. wt.% (Symbols as in Fig. 9).

From the results of the analyses, it could be concluded that the samples containing high silica content, and consequently low clay minerals content are characterized by a general depletion in the concentration of trace elements. On the other hand, distinctly enriched in most trace elements are those samples containing less silica and high clay mineral content. This confirms the close association of most of these trace elements with clay minerals. It is possible that the greater part of such trace elements have been inherited from the source rocks and bounded with the clay mineral lattices at or slightly after the mineral formation.

Generally, strontium shows the highest concentration (189.8 ppm in average) followed by V, Cr, Zn and then Cu. B, Ni and Co. Li and Pb show lesser values while Mo represents the least content, being less than 5 ppm in all the analyzed samples (Tables 2-6).

The geochemical correlation studied by El Shahat and El Sherbini (1994) suggested that **chromium** is mainly accommodated in the iron oxides and in clay minerals. This is indicated also by the strong positive correlation with Fe_2O_3 wt% in the majority of samples of the studied formations (Fig. 12, B-E). Chromium also shows positive correlation with a number of major and trace elements, which are closely associated with iron oxides and clays *e.g.* Ni, Co, Zn, Cu, Mn and Al.

Nickel shows strong sympathetic variation with Fe_2O_3 in four of the studied formations (Fig. 13, B-E), besides a large number of other elements, which are heavily loaded on iron oxides and clays. The geochemical behavior of Ni in the examined samples suggests a trend similar to that of Cr.

Copper relation with the other elements is similar to that observed in the behavior of Cr and Ni indicating their incorporation in the iron oxides and the clays. Copper shows strong positive correlation with Fe_2O_3 in all the studied samples (Fig. 14, A-E).

Zinc is particularly enriched in the analyzed samples; it reaches an average of 95.8 ppm. The relative enrichment of Zn is expected as the analyzed clayey samples have high content of iron oxides and clays, which easily accommodate the bulk of Zn. The geochemical behavior of Zn suggests a very strong positive correlation with Fe_2O_3 in all the studied samples (Fig. 15, A-E). Zn relation with the other elements points to its detrital nature in the examined samples. Wedepohl (1972) suggested that the major transport and accumulation of Zn in sedimentary environments occur mainly in the ferric oxides and clay minerals.

Strontium shows the maximum average in the analyzed samples, it reaches up to 189.8 ppm. It reaches the maximum values in all analyzed samples of the Daffin Formation (Table 6 and Fig. 16-E). The samples which are commonly
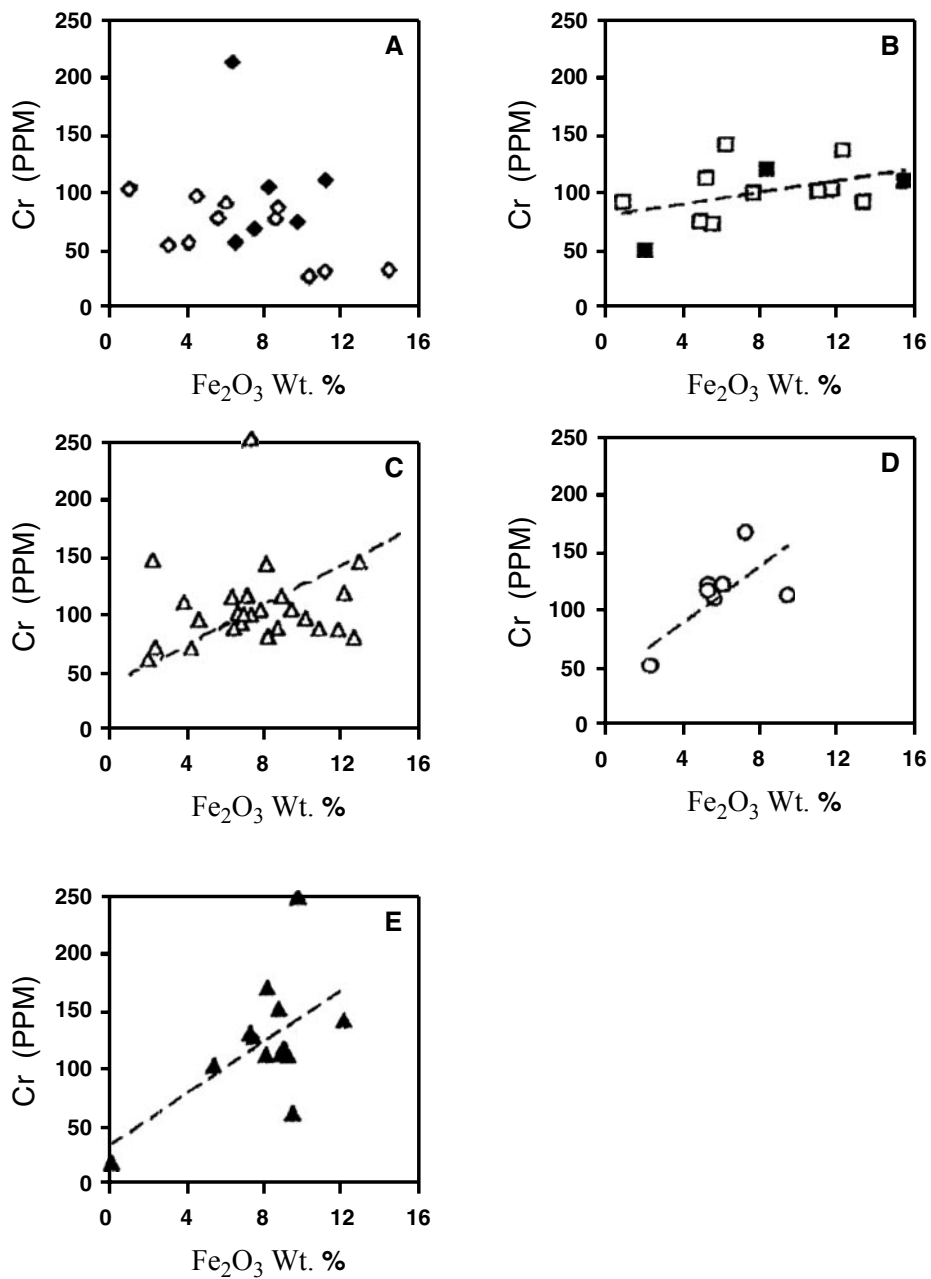
FIG. 12. Geochemical relationship diagrams (A-E) showing the effect of Fe_2O_3 wt.% on the distribution of Cr ppm (Symbols as in Fig. 9).
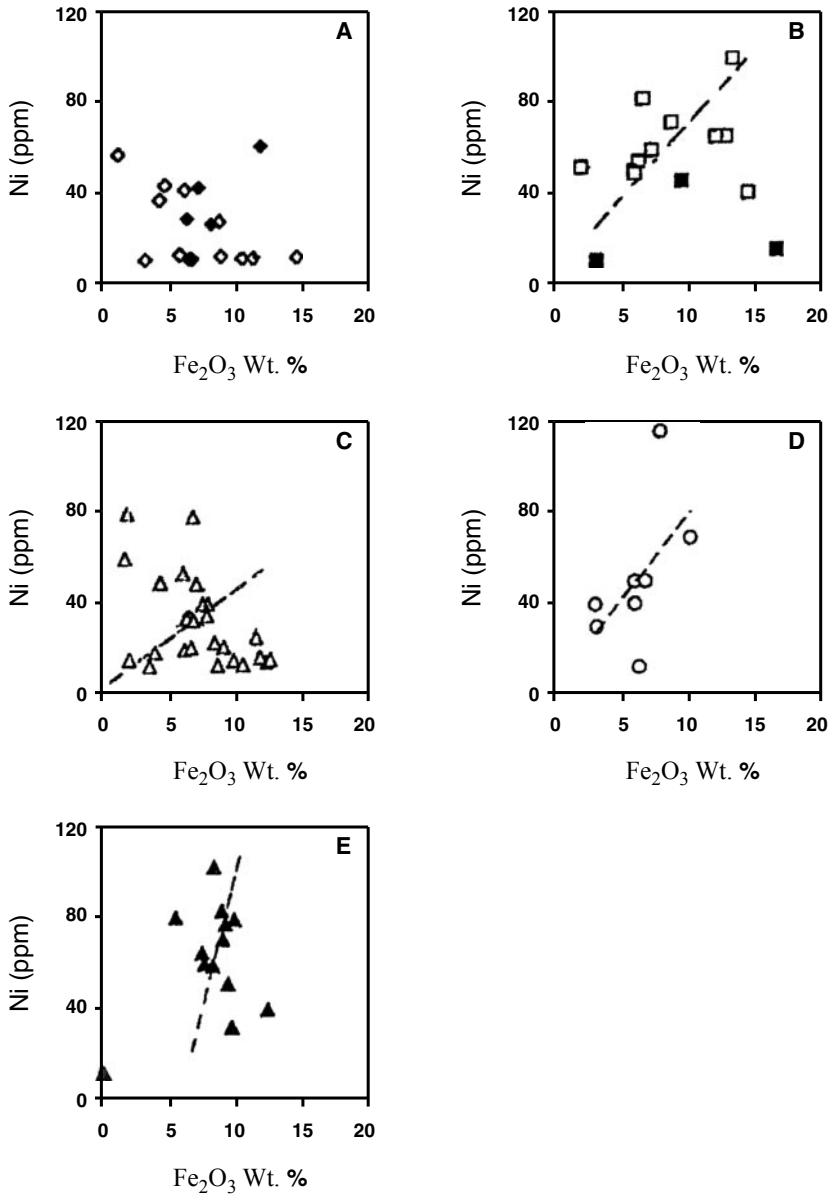
FIG. 13. Geochemical relationship diagrams (A-E) showing the effect of Fe_2O_3 wt.% on the distribution of Ni ppm (Symbols as in Fig. 9).
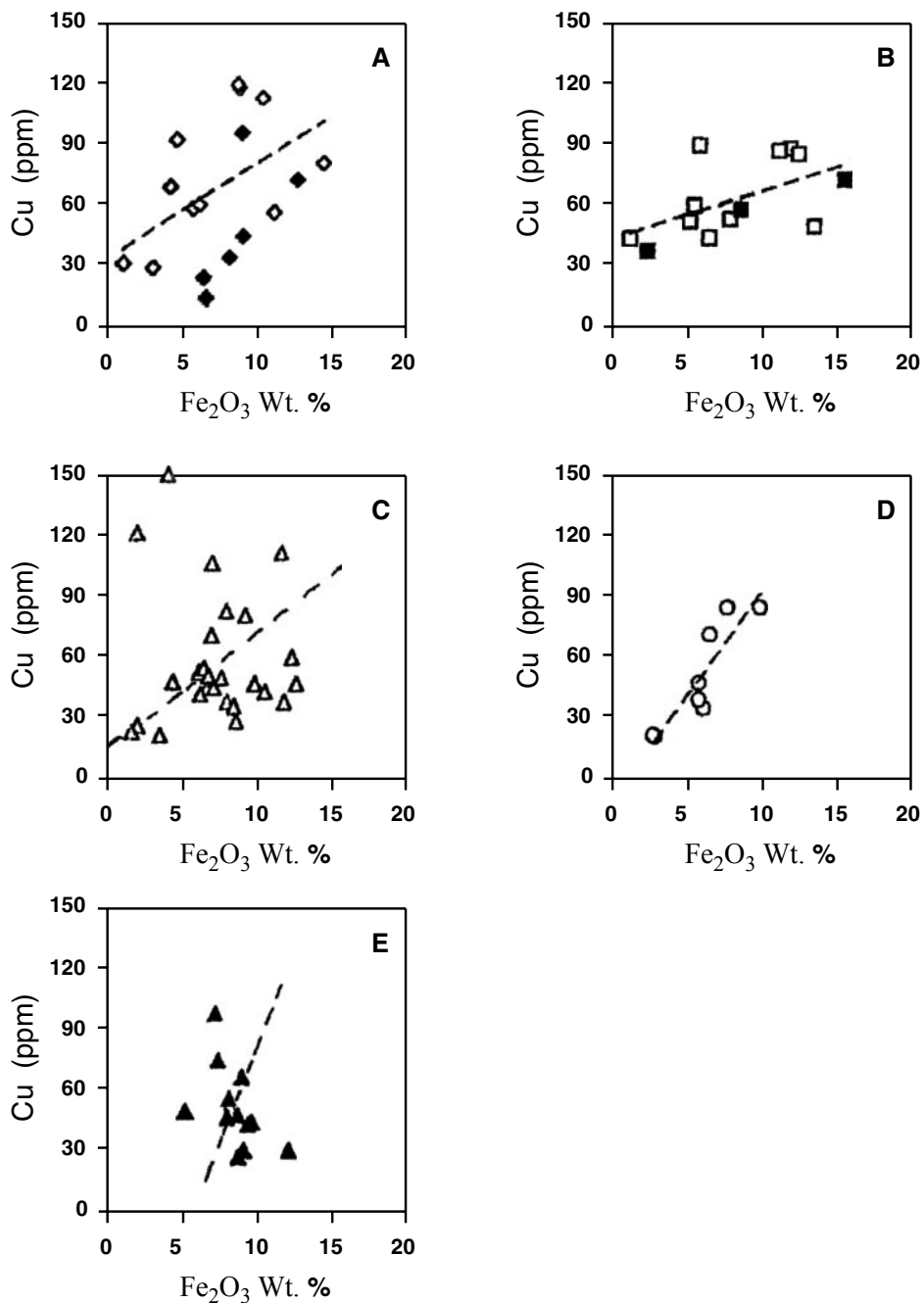
FIG. 14. Geochemical relationship diagrams (A-E) showing the effect of Fe_2O_3 wt.% on the distribution of Cu ppm (Symbols as in Fig. 9).
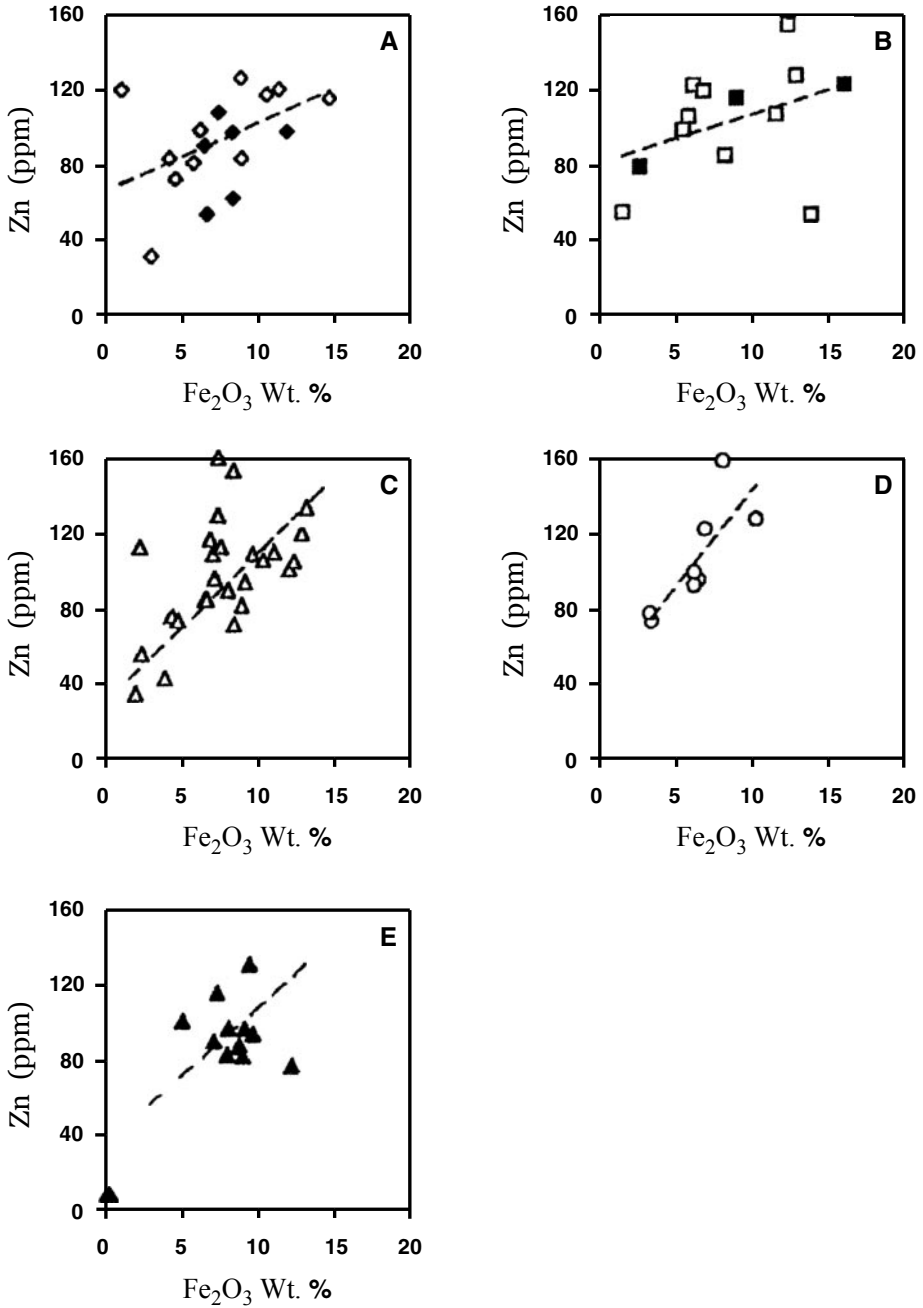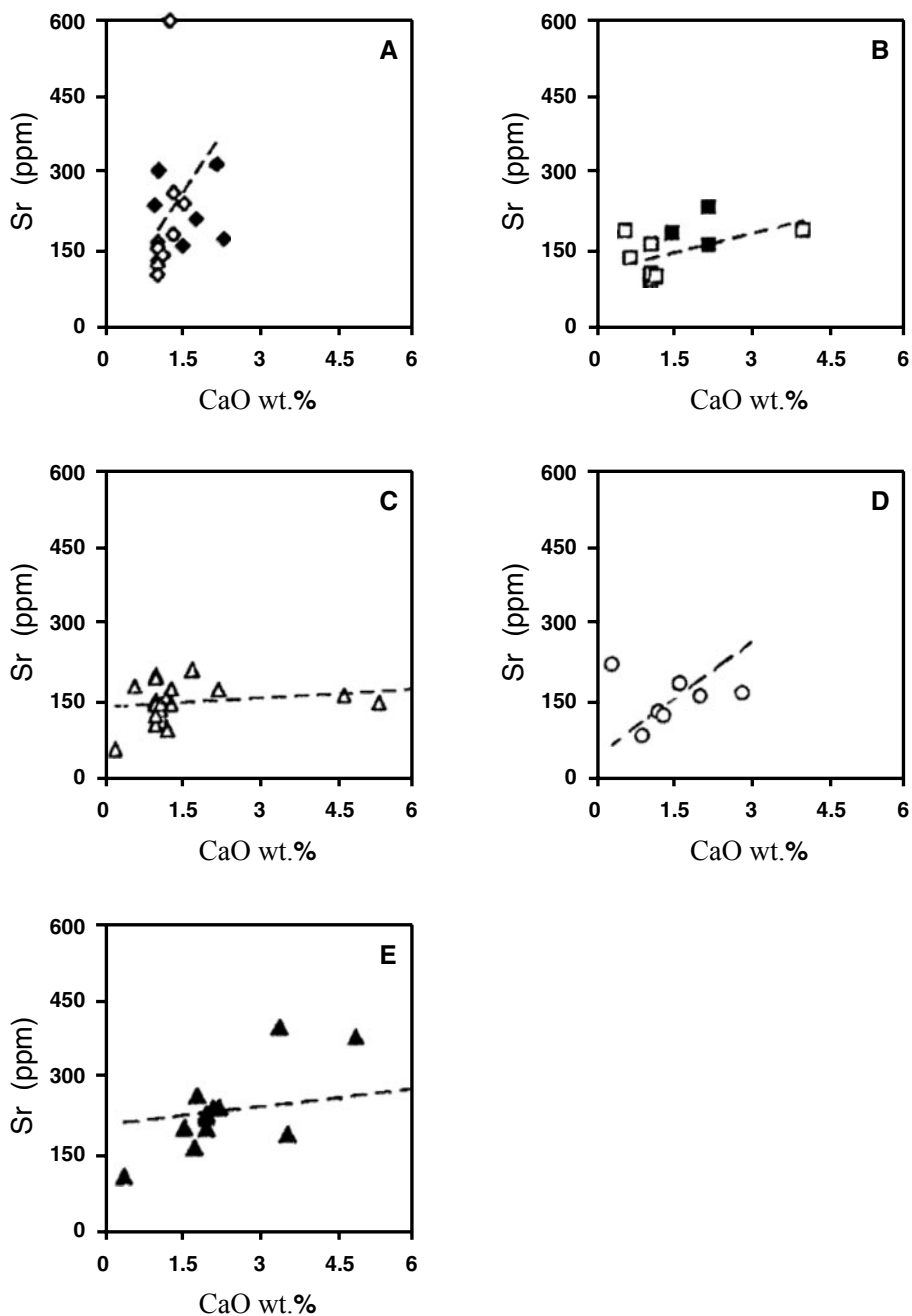
F<small>IG</small>. 15. Geochemical relationship diagrams (A-E) showing the effect of Fe_2O_3 wt.% on the distribution of Zn ppm (Symbols as in Fig. 9).

F IG. 16. Geochemical relationship diagrams (A-E) showing the effect of CaO wt.% on the distribution of Sr ppm (Symbols as in Fig. 9).

gypsiferous and calcareous have the highest levels of Sr. The latter has a strong sympathetic variation with CaO in all samples of the studied samples (Fig. 16, A-E), confirming its association with Ca-bearing minerals particularly calcite and gypsum. The fine dispersed carbonate particles within the clays acted as an accumulator for Sr, Ca, Mg and Sr are generally detritally with the carbonate content. Copper also correlates positively with CaO content. Both Sr and Cu are positively correlated with montmorillonite (*e.g.* Samples 63, 31, 40, 7, 9 & 91B in Tables 1, 2, 4 & 5). The high exchange capacity of montmorillonite, as well as the similarity of the ionic radius of Cu and Sr support their accommodation.

Lithium has a low average value in the analyzed samples (17.4 ppm). It is mainly accommodated in kaolinite, although the latter is not referred to as a Li-bearing mineral in text books of geochemistry. Kaolinite is regarded as Li-carrier in the Carboniferous sediments of Scotland (Wilson *et al*., 1972). Li-bearing kaolinite is largely attributed to its source rocks, that generally contain more Li-content as the granitic and some pelitic rocks. The leached acidic environment, in which kaolinite is mainly formed favors the Li-entrance into the kaolinite lattice to compensate the substitution of Mg^{2+} and /or Fe^{2+} for the octahedral Al^{3+}.

Gallium is present in clay minerals structure and it shows a proportional relation with Al_2O_3 in all samples of the studied samples (Fig. 17, A-F). It is noticed that Ga and Al_2O_3 are present in relatively higher content in Usfan and Shumaysi formations (Table 7 & Fig. 17, A-B) than in the other formations. However, the values of Ga and Al_2O_3 in Khulays Formation are fluctuated (Fig. 17 C).

Boron (10 to 157 ppm, Tables 2-6) is on the whole of the analyzed samples, much lower than 100 ppm which is that of the "average shale" of Turekian and Wedepohl (1961). The relatively high values are recorded in samples having more illite (*e.g.* Samples 62, 65, 66, 67 & 129 in Tables 1, 2, 4 cont. & 5). It is indicated by Harder (1970) that in marine sediments; B is enriched in illite rather than in kaolinite-montmorillonite-rich mudrocks. This fact is evidenced, to some extent, in the studied formations where B shows high values in samples having considerable illite content (Basyoni *et al*., 2002). Harder (Op. Cit.) attributed that the boron content in clays is due to a weakly bound either adsorbed B, or its incorporation in the structures of clay minerals.

Several trace elements are used as indicator elements in discriminating depositional environments. Degens *et al*. (1957) concluded that **B & Ga** are in relatively insoluble forms of combination and therefore they are suitable for use as paleosalinity indicators. The values of both trace elements are generally fluctuated in the analyzed samples.
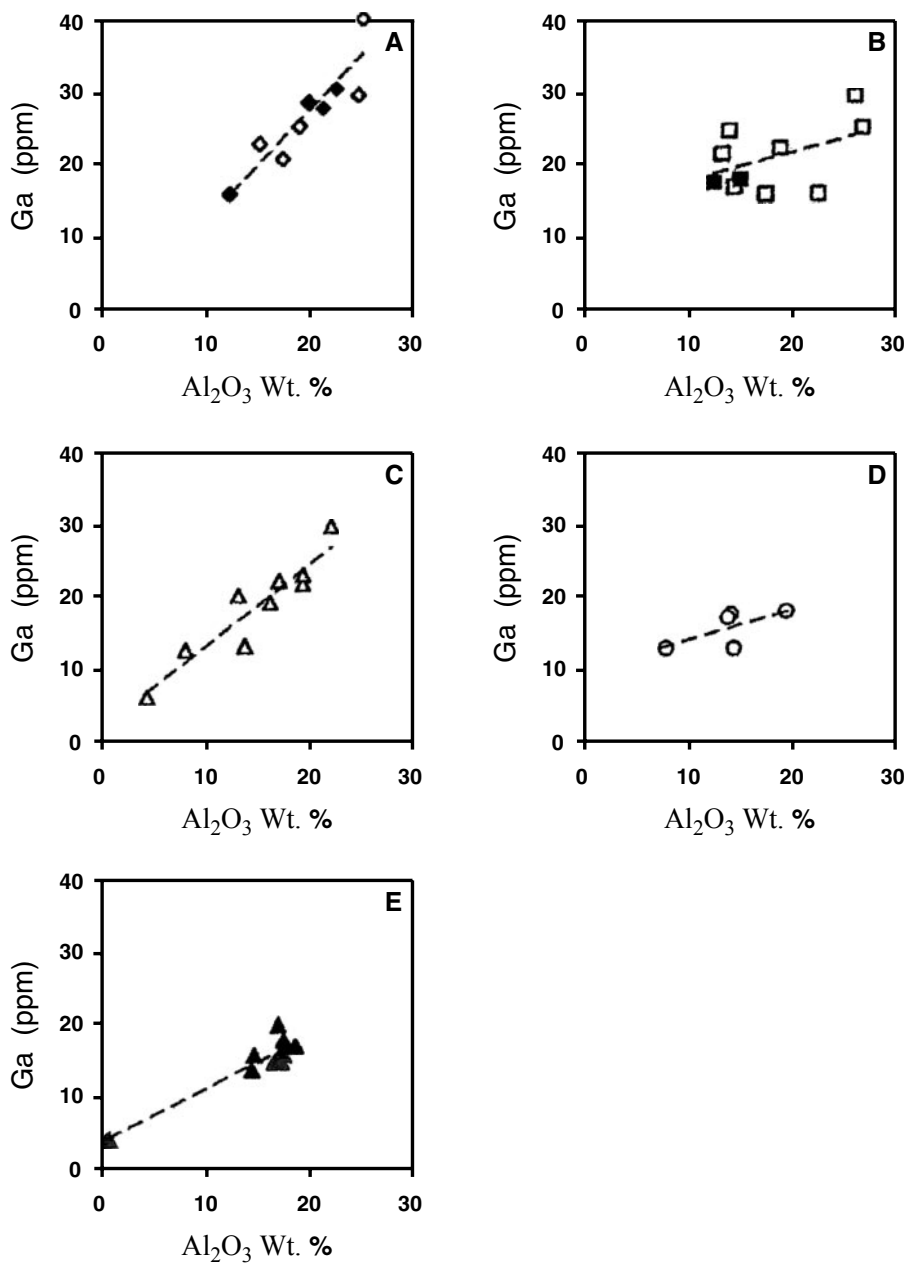
FIG. 17. Geochemical relationship diagrams (A-E) between Al_2O_3 wt% and Ga ppm in the analyzed clay and associated clays samples. (Symbols as in Fig. 9).

Boron and rubidium are more abundant in a group of marine shales rather than in a group of fresh-water shales of Pennsylvanian age, whereas Ga is more abundant in fresh-water group (Degens *et al*. 1957). In the present study, it appears possible by using the ternary diagram of Ga, Rb & B (Fig. 18) to indicate marine to transitional depositional environments for the clay deposits and associated mudrocks of the studied formations. Specifically; values of Shumaysi and Haddat Ash Sham formation are plotted in transitional environment field. However, those values of the other studied six formations indicate a marine depositional environment.
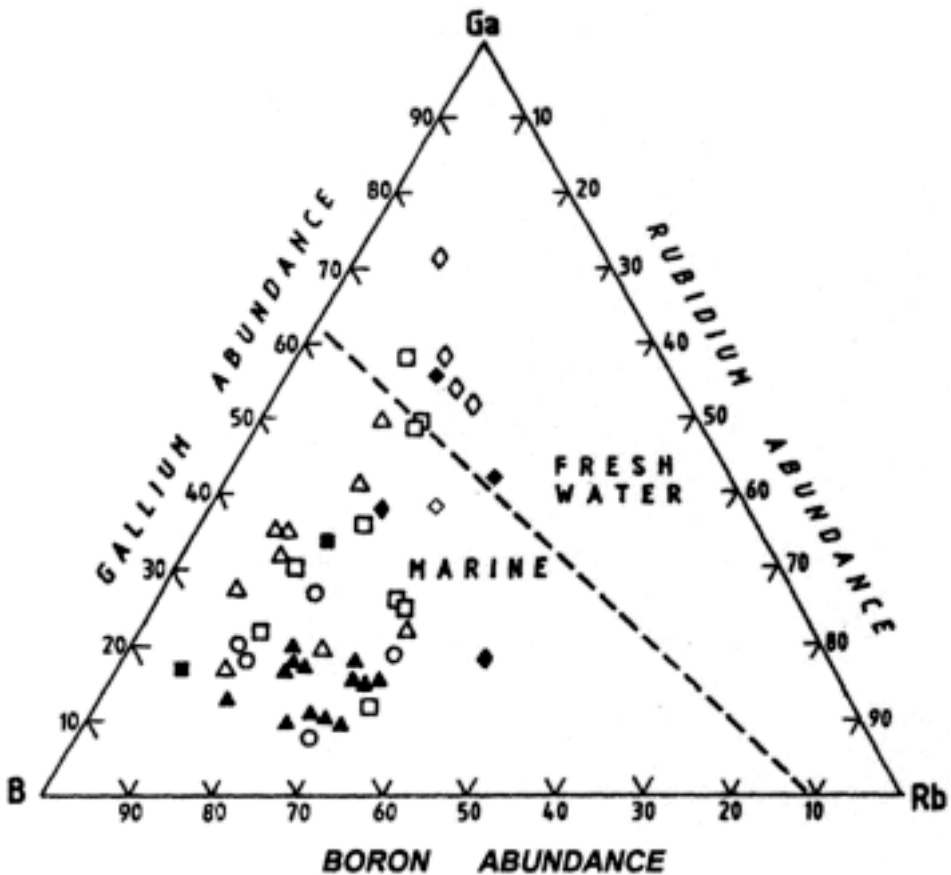
FIG. 18. Triangular diagram showing abundance of gallium, rubidium and boron in ppm, and depositional environments in forty seven samples of: Haddat Ash Sham ◆, Usfan ✧, Buraykah ■, Shumaysi ❏, Khulays △, Ubhur ○ and Daffin formations ▲ (after Degens *et al.,* 1957).

Co, Ni, Cr and V have diverse affinities and might partially belong to the detrital, organic, as well as the sulphide chemically precipitated components of sediments (Gindy and Tamish, 1985). Simple bivariate diagrams between **V & Cr** (Fig. 19, A-E) are established. These diagrams show one prominent cluster of plots mostly around one maxima, but some individual samples plots display, to some extent, diffuse or flat scatter. These maxima suggest little changes in the quality and/or provenance of detrital matter containing these elements and which was supplied to the depositional sites of the studied formations.

Bivariate plots between **Co & Ni** (Fig. 20, A-E) display a very diffuse or flat scatter, which could indicate a strong change in the quality and/or provenance of detrital matter containing these elements. Post-depositional mobility of these elements in intrastratal solutions of sediments of the depositional sites of the studied clays is thus suggested.

Conclusion

Chemical analyses for the relevant major oxides and elven trace elements: Li, B, V, Cr, Co, Ni, Cu, Zn, Sr, Mo and Pb were conducted on seventy-seven samples from the studied seven formations. However, Ga and Rb were carriedout on forty-seven samples selected from the same formations. The results show a wide range of variation in their major constituents and indicate a close association of most of the analyzed trace elements with the detritus clay minerals. Some of these elements are used as environmental discriminators. Based on the geochemical investigation, the following conclusions have been arrived at:

a – A positive correlation exists between Fe_2O_3 and each of MnO, Cr, Ni, Cu, and Zn; between Sr and Cu versus CaO; and also between Ga and Al_2O_3.

b – SiO_2 shows a negative correlation with each of Al_2O_3 and L.O.I. SiO_2 varies chiefly with relative amounts of either the detrital quartz grains or the other silicate minerals or both. The Al_2O_3 varies mainly according to the abundance and kind of clay minerals.

c – Most of trace elements are detritally associated and entered the depositional basin in close association with clay minerals and Ca-Fe-bearing detritus.

d – Although, the studied clay minerals and trace elements are mainly source controlled (*e.g.* granitic and some pelitic rocks represent the source of Li). Geochemical studies based on trace elements are performed since clay minerals contain the major part of such elements due to their reactivity, variability of structure and the very small grains size. Clay minerals and trace elements seem to be regulated and stabilized by depositional environment.

e – The distribution of Ga, B and Rb in a ternary diagram would indicate marine to transitional depositional enviroments for studied clay deposits. The diversity of clay minerals (kaolinite, montmorillonite, illite and chlorite, Table 1)
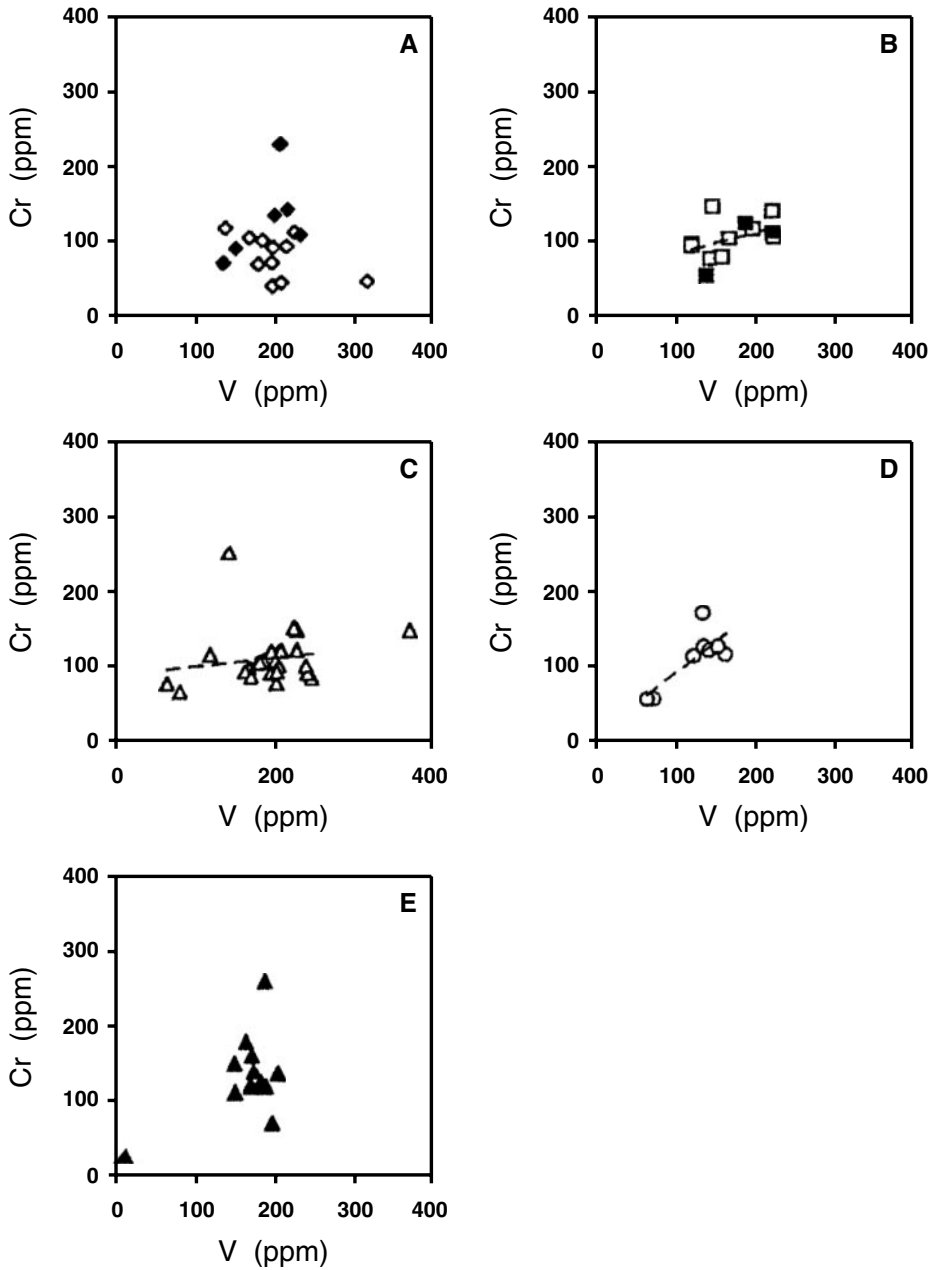
F IG. 19. Bivariate diagrams (A-E) of V vs Cr ppm for 77 analyzed samples of the studied formations. (Symbols as in Fig. 9).
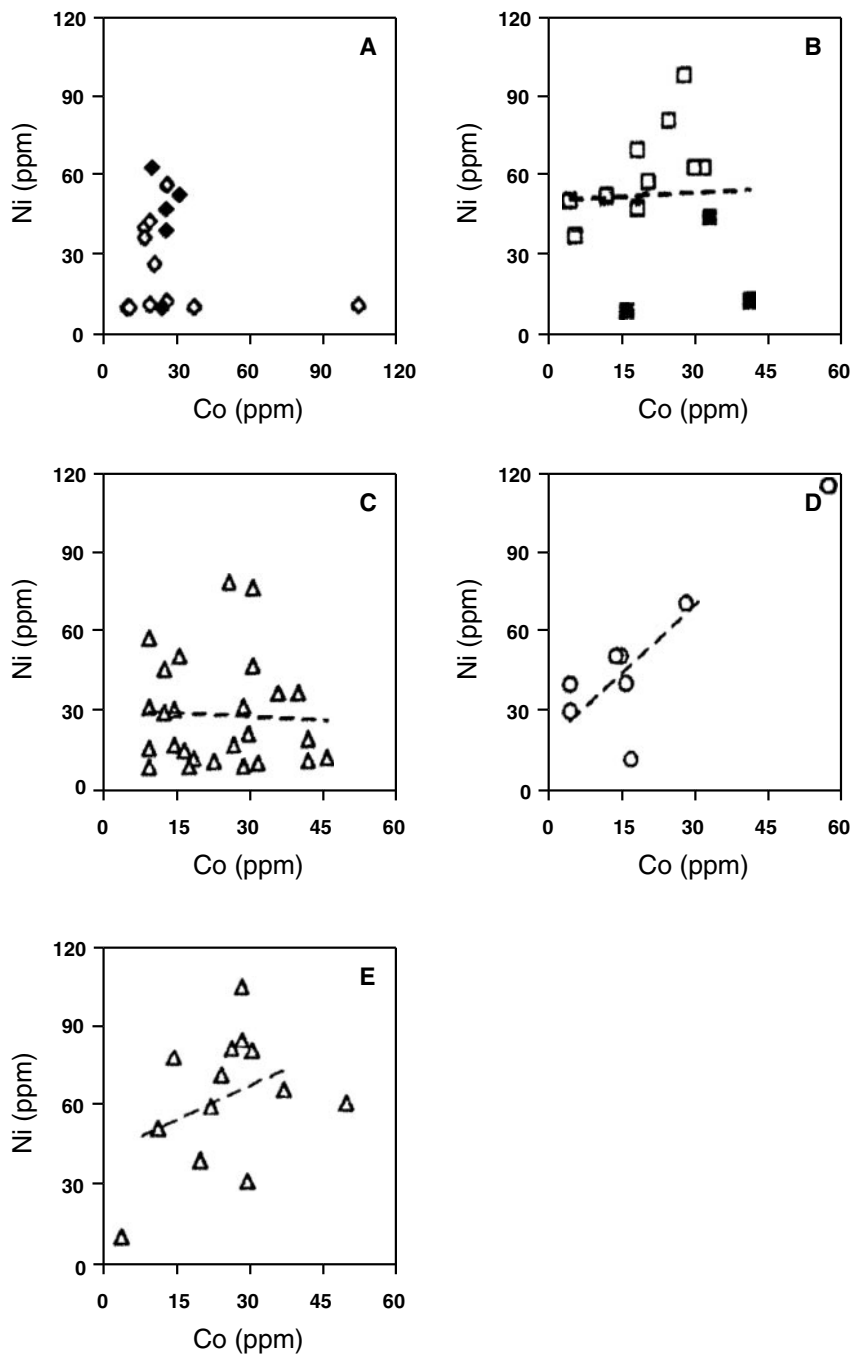
FIG. 20. Bivariate diagrams (A-E) of Co vs Ni ppm for 77 clayey analyzed samples of the studied
formations (Symbols as in Fig. 9).

and the different values of concentration of trace elements (Li, B, V, Cr, Co, Ni, Cu, Zn, Sr, Rb and Ga), besides, some elements show one prominent cluster of plots mostly around one maxima. All together suggest the possible source area of the studied clastic in the Arabian Shield. Their parental rocks are: low and high grade metamorphic rocks, igneous rocks (basaltic and granitic) and sedimentary rocks of pelitic nature.

Acknowledgment

References

Al-Shanti, A.M.S. (1966) Oolitic iron ore deposits in Wadi Fatima between Jeddah and Mecca, Saudi Arabia. *Saudi Arabian Dir. Gen. Min. Resources. Bull.* **2,** 51 p.

Basyoni, M.H., El-Askary, M.A., Saad, N.A. and **Taj, R.**J. (2002) Mineralogy of the Tertiary clay deposits in Makkah and Rabigh quadrangles, west-central Arabian Shield, Saudi Arabia. *Jour. Sci. Res., Sultan Qaboos Univ., Oman,* 7 **(2002):** 259-277.

Brown, G.F., Jackson, R.O., Bogue, R.G. and **Maclean, W.H.** (1963) Geology of the southern Hijaz quadrangle, Kingdom of Saudi Arabia. *Saudi Arabian Directorate General of Mineral Resources, Miscellaneous Geologic Investigations* **Map I-210A, 1:500,000 scale.**

Degens, E.T., Williams, E.G. and **Keith, M.L.** (1957) Enviromental studies of Carboniferous sediments, Part 1: Geochemical criteria for differentiating marine from fresh-water shales. *AAPG,* **41:** 2427-2455.

El Askary, M.A. and **El Mahdy, O.R.** (1976) The Nubia Sandstone at Kharga Oasis, a fresh water deposit: geochemical evidence. *Chemical Geology*, **17:** 1-11.

El Shahat, A. and **El Sherbini, M.I.** (1994) Mineral composition and trace elements distribution in the soils of the Nile Delta Environs. *Env. Sciences,* **7:** 69-87.

El Sherbini, M.I. (1995) Clay mineralogy and geochemistry of the Neogene- Quaternary subsurface Nile Delta sediments, Egypt. *Bull. Fra. Sci., Mansoura Univ.,* **22**(1**)** 233-257.

Gindy, A.R. and **Tamish, M.O.** (1985) Some major and trace constituents of Phanerozoic Egyptian mudrocks and marls. *Jour. African Earth Sciences*, **3:** 303-320.

Harder, H. (1964) Kohlensauerlinge als eine Eisenquelle der sedimentaren Eisenerze. In: *G.O. Amstutz* (editor), *Sedimentology and Ore Genesis, Elsevier, Amsterdam,* 107-112.

Harder, H. (1970) Boron content of sediments as a tool in facies analysis. *Sediment.* ***Geol.,*** **4**: 153-175.

Karpoff, R. (1975) Esquisse geologique d'Arabie Saoudite. *Bull. de la Societe Geologique de France* **(6), VIII:** 653-693.

Keith, M.L. and **Degens, E.T.** (1959) Geochemical indicators of marine and fresh water sediments. In: *P.H. Abelson* (editor), *Research in Geochemistry, Wiley & Sons, New York,* 38-61.

Moore, T.A. and **Al-Rehaili, M.H.** (1989) Explanatory notes to the geologic map of the Makkah Quadrangle. **Sheet 21D,** Kingdom of Saudi Arabia. *DGMR,* Jeddah, Saudi Arabia.

Pallister, J.S. (1982) Reconnaissance geologic map of the Harrat Tuffil quadrangle, sheet 20/39B, Kingdom of Saudi Arabia. *Saudi Arabian Deputy Ministry for Mineral Resources, Open-File Report* **USGS-OF-03-33,** no text, map 1:100,000 scale.

Pallister, J.S. (1986) Geologic map of the Al Lith quadrangle, sheet 20D, Kingdom of Saudi Arabia. *Saudi Arabian Deputy Ministry for Mineral Resources,* **Geoscience map GM-95,** 1:250,000 scale.

Ramsay, C.R. (1986)Geologic map of the Rabigh quadrangle. *Sheet 22D,* Kingdom of Saudi Arabia. **Geoscience map GM-84C,** 1:250,000 scale.

Saad, N.A. (1996) Conditions controlling the clay mineralogy of mudrocks in some localities of the Western Desert of Egypt. *Bull. Fac. Sci., Alex. Univ.,* **36**(2): 401-426.

Sorem, R.K. and **Gunn, D.W.** (1967) Mineralogy of manganese deposits, Olympic Peninsula, Washington. *Econ. Geol.,* **62:** 22-56.

Spencer, C.H. and **Vincent, P.L.** (1984) Bentonite resources potential and geology of Cenozoic sediments, Jeddah region. *Saudi Arabian Deputy Ministry for Mineral Resources, Open-File Report* **BRGM-OF-04-31,** 60 p.

Taj, R.J., El Askary, M.A., Saad, N.A. and **Basyoni, M.H**. (2001a) Sedimentology, mineralogy, chemistry and industrial applications of argillaceous rocks in some localities in Makkah and Rabigh quadrangles, west central Arabian Shield, Saudi Arabia. *Sponsored research study by King Abdulaziz University,* **Project No. 203/419, final report,** 228 p.

Taj, R.J., El Askary, M.A., Saad, N.A. and **Basyoni, M.H.** (2001b) Eonomic potentiality of the Tertiary clay deposits in Makkah and Rabigh quadrangles, west-central Arabian Shield, Saudi Arabia. *5th Int. Conf. on Geochemistry, Alex. Univ., Egypt,* **2:** 169-183.

Taj, R.J., El Askary, M.A., Saad, N.A. and **Basyoni, M.H.** (2002) Mineralogical investigation and some sedimentary phenomena of Ubhur Formation, north Jeddah, Saudi Arabia. *Jour. Marine Sciences, King A. Aziz Univ., Jeddah,* **13:** 93-110.

Tosson, S. and **Saad, N.A.** (1974) Genetic studies of El-Bahariya iron ore deposits, Western Desert, Egypt. *N. Jb. Miner. Abh.,* **121**(3): 293-317.

Turekian, K.K. and **Wedepohl, K.H.** (1961) Distribution of trace elements in some major units of earth's crust. *Bull. Geol. Soc. Am.,* **72:** 172-192.

Wedepohl, K.H. (1972) Zinc In: Handbook on geochemistry (ed. Wedepohl, K.H.). Springer-Verlag, Berlin, 2, 30 K1-30K13.

Wilson, M.J., Bain, D.C., McHardy, W.J. and **Berrow, M.L.** (1972) Clay-minerals studies on some Carboniferous sediments in Scotland. *Sed. Geol.,* **8:** 137-150.

Zeidan, R. and **Banat, K.** (1989) Petrology, mineralogy and geochemistry of the sedimentary formations in Usfan, Haddat Ash-Sham and Shumaysi areas, and their associated oolitic ironstone interbeds, northeast and east of Jeddah, Saudi Arabia. *Sponsored Research study by King Abdulaziz University,* **Project No. 035/406, final report**, 264 p.

جيوكيميائية وبيئات ترسيب الرواسب الطينية في العصر الثالث بمربعي مكة ورابغ، غرب وسط الدرع العربي، المملكة العربية السعودية

رشدي جمال تاج*، نادي أديب سعد**، محمد أبواليزيد العسكري**،
محمد حسين بسيوني*

*كلية علوم الأرض ، جامعة الملك عبد العزيز ، جـــدة – المملكة العربية السعودية

**قسم الجيولوجيا ، كلية العلوم ، جامعة الإسكندرية

الإسكنـــدرية – جمهورية مصر العربية

المستخلص. يقدم هذا البحث دراسة كيميائية مستفيضة لصحبات معادن الطين المميزة لبعض رواسب الطين والطفلة والصخور الطينية، والتي تختلف في أنسجتها ولونها وخواصها الصخرية. وقد اختير للدراسة عينات تم جمعها من سبعة متكونات مختلفة تنتمي إلى العصر الثالث وتقع جميعها في مربعي مكة ورابغ بالجزء الغربي الأوسط من المملكة العربية السعودية. وشملت التحاليل الكيميائية أكاسيد العناصر الأساسية وبعض العناصر الشحيحة لعدد سبعة وسبعين عينة، وقد أظهرت النتائج تغيرات كبيرة في العناصر الشائعة والشحيحة بالعينات المدروسة. ويعزى الاختلاف الكبير في المحتوى الكيميائي إلى الاختلاف في نوعية ووفرة المعادن الطينيـة أو قلة من المواد المختلطة الأخرى مثل الكوارتز المنقول، الفلسبار وبعض المعادن الثقيلة. ومن المؤثرات الأخرى المسببة لهذه الاختلافات التواجدات المحلية لعريقات الكربونات والقليل من الجبس في بعض المتكونات والمواد الحديدية في متكونات أخرى.

وتوصل البحث إلى بعض الاستنتاجات الهامة معتمدا على الدراسات الجيوكيميائية ودراسة توزيع العناصر الرئيسية والشحيحة وهذه الاستنتاجات هي:

أ – علاقات ارتباط موجبة في بعض المتكونات بين أكسيد الحديديك

وكل من أكسيد المنجنيز، الكروم، النيكل، النحاس، الزنك وأيضا بين الاسترونشيوم والنحاس مقابلا لأكسيد الكالسيوم وفي معظم الأحيان بين الجاليوم و أكسيد الألومونيوم.

ب – تظهر السيليكا علاقة ارتباط سالبة مع كل من أكسيد الألومونيوم وفاقد الحرق.

ج – معظم العناصر الشحيحة المصاحبة منقولة، وقد دخلت أحواض الترسيب في علاقة وثيقة مع معادن الطين والرواسب المنقولة الاخرى الحاملة للكالسيوم والحديد. ويرجع الاختلاف في نوعية وكميات المعادن الطينية وماتحتويه من عناصر شحيحة إلى اختلاف صخور المصدر مثل الصخور الجرانيتية وبعض الصخور الطينية.

د – من العلاقات الثنائية بين البورون والجاليوم، والعلاقة الثلاثية بين الجاليوم والبورون والربيديوم أمكن استنتاج أن رواسب الطين والصخور الطينية المصاحبة للمتكونات المختلفة قد ترسبت في بيئات تتراوح بين البيئتين البحرية والانتقالية.

الكلمات الدالة : رواسب طين العصر الثالث ، مربعي مكة ورابغ ، المملكة العربية السعودية ، جيوكيميائية وبيئات ترسيب .